DOI:
10.1002/stem.2895

Document Version
Peer reviewed version

Molecular programming of perivascular stem cell precursors

Val Yianni and Paul T Sharpe

Centre for Craniofacial and Regenerative Biology, Dental Institute, Kings College London

Address for correspondence: Paul Sharpe, CCRB, Dental Institute, Kings College London, Floor 27 Guys Hospital, London SE1 9RT. Paul.sharpe@kcl.ac.uk

Keywords: Pericyte, adult stem cells, MSC, epigenetics, transcriptomics

Author Contributions: Val Yianni carried out the experiments. Paul Sharpe was responsible for the experimental design. Both authors wrote the manuscript.

Abstract

Pericytes have been shown to act as precursors of resident adult stem cells in stromal tissues *in vivo*. When expanded *in vitro* these cells are capable of giving rise to multiple mesenchymal cell types, irrespective of their tissue of origin. This phenomenon of multi-lineage differentiation is only observed in culture, whereas *in vivo*, stromal stem cell differentiation is restricted to tissue-specific cell types. An important unanswered question is how a single, widely distributed cell type (a pericyte), gives rise to stem cells with tissue-specific functions and attributes. Using a combination of transcriptomics and epigenomics we have compared the molecular status of two populations of stromal stem cell precursors. By utilising a LacZ transgene insertion that is expressed in pericytes but not in stem cells, we were able to compare pericyte populations from two different tissues, mouse incisors and bone marrow. Pericytes, freshly isolated from mouse incisors and bone marrow exhibited transcriptomes and epigenetic landscapes that were extensively different, reflecting their tissue of origin and future *in vivo* differentiation potential. *Dspp*, an odontoblast differentiation gene, as well as additional other odontogenic genes are shown to be expressed in dental pulp-derived pericytes. These genetic loci are also decorated with histone modifications indicative of a transcriptionally active chromatin state. In bone marrow pericytes a major osteogenic differentiation gene, *Runx2* is not expressed but is marked by both active and repressive histones and therefore primed to be expressed. Polycomb Repressor Complex 1 (PRC1), analysis showed that key genes involved in the induction of adipogenesis, chondrogenesis and myogenesis are targeted by Ring1b and therefore stably repressed. This indicates that pericyte populations are molecularly obstructed from differentiating down certain lineages *in vivo*.

Introduction

Stem cells are present in the stroma of adult tissues and organs and are known by a variety of generic and tissue specific names, including, stromal stem cells, mesenchymal stem cells, skeletal stem cells, dental pulp stem cells etc. (Hematti & Keating, 2010; Jiang et al., 2002). Originally isolated from bone marrow, these cells have been extensively characterised *in vitro* where a set of criteria are used to define a cell population as having stem cell properties. Fundamental among these is the stimulation of differentiation *in vitro* down osteogenic, chondrogenic and adipogenic pathways. Addition of specific cocktails of factors to these stem cells in monolayer culture can stimulate differentiation down these three lineages that are conventionally assayed by marker gene expression and/or histological staining for mineral, proteoglycans and lipids (Huang, Gronthos, & Shi, 2009; Phinney & Sensebé, 2013). This tri-lineage differentiation property of the stem cells isolated from different tissues is however a uniquely *in vitro* property that has yet to be observed for any population *in vivo*. *In vivo*, differentiation is restricted to a single cell type, appropriate to their tissue of origin and inappropriate differentiation is considered a pathological/disease condition (Diaz-Flores et al., 2009; Jifan Feng et al., 2011; Vidovic et al., 2017).

Numerous studies have implicated perivascular cells (hereafter referred to as pericytes), as a likely common source of stem cell precursors in multiple tissues (Crisan et al., 2008; da Silva Meirelles, Chagastelles, & Nardi, 2006; Shi & Gronthos, 2003). *In vitro* studies showed that cultured pericytes, from multiple organs showed some of the cardinal properties of stem cells including their immunophenotype and broad differentiation potential (Bexell et al., 2009; Brighton et al., 1992; Covas et al., 2008; Crisan et al., 2008). Crisan et al (2008) demonstrated that human perivascular cells, isolated and expanded in culture express typical markers ascribed to stromal/mesenchymal stem cells, including CD73, CD44, CD105,

and CD90. Pericytes *in vivo* have been shown to express MSC markers including CD73, CD44, CD105, and CD90 (Feng-Juan lv, Tuan, Cheung, & Leung, 2014). In addition, perivascular cells have been detected in virtually all organs *in vivo* based on their close association with blood vessels, where they express a combination of markers such as CD146, NG2, PDGFR-Rβ, and α-SMA. Several cre mouse lines for these markers have been used with reporter lines to trace pericytes during tissue/organ growth and repair. Using these lines a common origin of stem cells has been established in several tissues using the gold standard of genetic lineage tracing. Pericytes have been shown to act as MSC precursors and give rise to follicular dendritic cells (Krautler et al 2012), white adipocytes (Tang et al 2008) and skeletal muscle (Dellavalle et al 2007). In tooth pulp, $NG2^+$ pericytes form a highly specialised tooth-specific cell type, odontoblasts during incisor growth and repair as do αSMA^+ pericytes in molar repair (Jifan Feng et al., 2011; Vidovic et al., 2017). In bone marrow, lineage tracing of osteoblasts using an Osx-Cre during early development showed that their precursors in developing bone migrate into the primary ossification centre with invading blood vessels in a pericyte-like manner and these cells also express PDGFR- β (Maes et al. 2010). The ubiquitous nature of pericytes as cells required to maintain blood vessel wall integrity suggests that in their role as stem cell precursors their differentiation *in vivo* must be regulated in some way to ensure appropriate differentiation.

Using a combination of transcriptomic profiling, and epigenetic characterisation of histone landscapes, we set out to determine the extent to which pericytes from different tissues are "molecularly programmed" to undergo restricted differentiation *in vivo* before they become stem cells. In order to do this we needed to separate pericytes from stem cells and since expression of the majority of surface markers is shared by both cell types we took advantage of a mouse transgene insert that drives β-galactosidase expression in pericytes in

multiple tissues but is not expressed in stem cells (Tidhar et al., 2001). We purified pericytes from two tissues bone marrow and incisor tooth pulp that share characteristics of high turnover rates and producing cells (osteoblasts and odontoblasts respectively) involved in mineralisation. These pericytes were subjected to RNA-Seq and epigenomic profiling without an *in vitro* cell culture step. Analysis of the datasets reveals extensive differences between the two cell populations that reflect their anatomical origins, *in vivo* function, and most importantly highlights mechanisms whereby pericytes are innately restricted in their available stem cell differentiation pathways depending on their tissue of origin. Thus pericytes contain a pre-programmed epigenetic landscape and transcriptome that anticipates their tissue specific function as stem cells.

Materials and Methods

Tissue Isolation. Homozygous *XlacZ4* (JAX: 018625, B6.FVB-Tg(Fabp4-lacZ)4Mosh/J) pups were collected at postnatal days 5 to 7 and sacrificed. Incisors were extracted from the mandible and maxilla and the tibia and femurs removed and placed into ice cold sterile phosphate buffered saline (PBS). The epithelium was removed from incisors using a fine needle and the remaining dental pulp placed in freshly made SB buffer (1% FBS, 10mM HEPES buffer pH7, PBS). The tissue was then isolated by centrifugation (1min x 12,000g), cut into small pieces using fine scissors and re-suspended in 5ml of Collagenase D (Roche, 11088866001) and Dispase (Stem cell technologies, 07923) . The tissue was allowed to dissociate by incubating the suspension in a cell culture incubator at 37^{o} in 5% CO_2. Cells from bone were extracted by flushing the marrow with SB buffer using a U100 insulin needle. Cells were then pelleted by centrifugation (5mins x 12,000g), the cell media removed and the pellet re-suspended in 200µl of ice cold SB buffer.

Histology. Cryosections were processed for Xgal staining as described in (J Feng, Mantesso, De Bari, Nishiyama, & Sharpe, 2011). Primary antibodies were used at a concentration of 1:1000, and biotinylated secondary antibodies used at a concentration of 1:500. Antibodies used were: rabbit anti CD146 (abcam, 75769), rabbit anti CD105 (abcam, 11414), rabbit anti α-smooth muscle actin (abcam, 5694), rabbit anti Collagen IV (abcam, 6586), rabbit anti NG2 (abcam, 129051), biotinylated anti rabbit IgG (Vector laboratories, BA-1000).

***Flow Cytometry*.** The dissociated tissue suspension was stained for β-galactosidase activity using the Fluorescein Di-β-D-Galactopyranoside system (Invitrogen, D2920) as per the manufacturer's instructions. Cells were then run through a BD FACS Aria III fusion machine, and flow cytometry analysis performed on a BD LSR Fortessa machine. Data analysis was

done with FlowJo v10 software. For flow cytometry analysis, cells were re-suspended in 100µl SB buffer (1% FBS, 10mM HEPES buffer pH7, PBS) and incubated with an appropriate antibody (1:100 concentration) for 60 minutes on ice. Antibodies used were the following: Rat mAb anti CD105 (ThermoFisher Scientific, 12-1051-82), Rat mAb anti CD90 (R&D, FAB7335P), Mouse mAb anti SSEA4 (R&D, FAB1435P), Rat mAb anti CD140b (eBioscience, 17-1402-82), Mouse mAb abti CD146 (eBioscience, 12-1469-41) and Rabbit mAb anti Annexin V (Abcam, ab108194).

RNA-isolation & RNA-seq analysis. Pericytes were isolated as previously described and total RNA was obtained using the "Quick- RNA MicroPrep" kit (Zymo Research, R1051) according to manufacturer's instructions. Following poly-A selection, cDNA libraries were generated using SMARTer (Clontech, 634925). Barcoded libraries were then pooled and sequenced on an Illumina Hiseq 4000 (75bp, paired end) at the Wellcome Trust Centre for Human Genetics (Oxford, United Kingdom). Raw reads were mapped to GRCm38/mm10 using Hisat2, and Deseq2 together with the Cufflinks pipeline were used to identify genes with differential gene expression. Feature counts was also used to generate count tables for every sample. A gene was classified as being differentially expressed if it had a q-value <0.05. All ChIP-seq and RNA-seq data are deposited under Bioproject number : PRJNA420442 in the NCBI (SRA) database. The following algorithms were used for RNA-seq and ChIP-seq data analysis: HISAT2 (D. Kim, Langmead, & Salzberg, 2015), DESeq2 (Love, Huber, & Anders, 2014), FeatureCounts (Liao, Smyth, & Shi, 2014), the Galaxy platform (Afgan et al., 2016), Cufflinks (Trapnell et al., 2012), DeepTools2 (Ramírez et al., 2016), Bowtie2 (Langmead, Trapnell, Pop, & Salzberg, 2009) and MACS2 (Zhang et al., 2008)

***Chromatin immunoprecipitation & ultra-low ChIP-Seq*.** Pericytes were FACS isolated from P5 XLacZ4 pups as described above. Freshly isolated cells (~10,000) were crosslinked, their chromatin

isolated, sheared and then precipitated using a suitable antibody for modified histones or chromatin binding protein of interest. ChIP-Seq libraries were generated using the "MicroPlex Library preparation Kit" (Diagenode, C05010012) and sequenced on an Illumina HiSeq 2000 sequencer (50bp paired-end). Sequencing was performed at the Wellcome Trust Centre for Human Genetics (Oxford, United Kingdom). The reads were firstly aligned to the mouse reference genome (GRCm38/mm10) using Bowtie2. Any reads not mapping uniquely to a locus were excluded from subsequent analysis. Peak calling was performed using MACS2 using a P-value cut-off of $p< 0.005$. For visualization purposes, ChIP-seq sample bedgraph files were normalized to input bedgraph files using DeepTools. The following antibodies were used for ChIP-seq: Rabbit pAb anti H3K27me3 (Active motif, 39155), Rabbit pAb anti H3K4me3 (Active motif, 39915) and Rabbit mAb anti Ring1B (Active motif, 39663).

In vitro pericyte culture and quantitative PCR. Pericytes from incisor pulp and bone marrow stroma were isolated as described. Tissue culture plates were coated with 0.1% gelatin (Sigma, G1393) and FACS isolated pericytes were seeded at a density of $1x10^4$/cm2. RNA was collected from cells as previously described after 31 days in culture. cDNA was synthesized using the NanoScript2 Reverse transcription kit (PrimerDesign). Quantitative RT-PCR was performed using the Precision qPCR master mix (PrimerDesign). The quantification cycle threshold values were normalized to the housekeeping gene (*Gapdh*) and ΔCq and ΔΔCq were calculated between samples and controls. The following Qiagen QuantiTect oligonucleotide primers were used: *Dspp* (QT00312228), *Pparγ* (QT00100296), *Runx2* (QT00102193), *Gapdh* (QT01658692), *Ibsp* (QT00115304), and *Col2a1* (QT01055523).

Results

Characterisation of dental pulp and bone marrow XlacZ4^{+} cells confirms their identity as pericytes. In order to compare the expression of cell surface markers associated with pericytes, LacZ^{+} cells in XlacZ4 transgenic mice were isolated from dental pulp and bone marrow and assayed using flow cytometry. The XlacZ4 line contains a random integration of a β-galactosidase gene cassette downstream of the αSMA gene locus (Tidhar et al., 2001), making β-galactosidase expression highly restricted to pericytes (Fig. S4 A). When assayed, ~1.3% of all cells derived from incisor pulp were LacZ^{+} pericytes and ~5.5% of all cells from bone marrow aspirate were LacZ^{+} (Fig. 1A & B). The percentages of LacZ^{+} cells expressing five commonly-used pericyte marker genes, PDGFRβ (Hellström, Kalén, Lindahl, Abramsson, & Betsholtz, 1999), CD146 (Feng-Juan lv et al., 2014), Endoglin (Dominici et al., 2006), Annexin A5 (Brachvogel et al., 2005) and SSEA4 (Gang, Bosnakovski, & Figueiredo, 2007) were found to be similar in LacZ^{+} cells of dental pulp and bone marrow (Fig. 1C & D). The percentage of cells positive for these markers were consistent between biological replicates (Fig. 1E). Although none of the markers used were present on 100% of the cells, as expected, the distributions between the two cell populations was suggestive of similar cell populations in the two different tissues. The only cells we could detect that were positive for *LacZ* were always attached to blood vessels in our organs of interest (Fig S1 A). LacZ^{+} cells were not found to express vascular endothelial markers such as *Cdh5*, *Kdr*, *Pecam1* or *Nos3* (Wang, Chen, & Zhang, 2016) (Fig. S1 B), nor the more recently proposed pericyte markers *Tbx18* (Guimarães-Camboa et al., 2017).

RNA-seq profiling of pericytes reveals unique transcriptomic signatures in bone marrow and dental pulp pericytes. Bulk RNA-seq was performed on fresh LacZ^{+} pericytes collected from dental pulp and bone marrow and RNA isolated without a prior *in vitro* expansion step.

Unsupervised hierarchal clustering which takes into account the transcriptome of cells as a whole, showed that biological replicates were more transcriptomically similar to pericytes from the same anatomical location than from different locations (Fig. 2A). DESeq2 analysis on the datasets showed that at an FDR < 0.05, 850 genes were significantly upregulated in dental pulp pericytes while 1000 genes were significantly upregulated in bone marrow pericytes (Fig. 2B). The majority of genes detected (approximately 3500) were transcribed in both populations and did not show any significant difference in their levels of transcription. Enrichment analysis on these shared genes showed that they encode proteins involved in regulation of mRNA processing, RNA splicing, translocation and various other homeostatic processes (Fig. 2C).

When considering functional categories of genes that were over-represented, several significant differences became clear recognising the extent that gene expression in pericytes reflected functions as mesenchymal stromal cells. Enriched gene sets for pericytes isolated from incisor pulp included hedgehog signalling & regulation of signalling via Smoothened (Fig. 3A). Core enrichment was detected in a number of hedgehog related signalling genes including transcription factors: *Gli1*, *Gli2*, *Gli3*, and receptors *Ptch2, Smo* and others (Fig. 3A') that are driving this over-representation. In addition, we surprisingly detected over-representation of genes that have been classically associated with odontogenesis (Fig. 3B). A significant number of genes were driving this core enrichment, 75 of which are shown with their relative expression values (Fig. 3B'). These included *Gli1*, *Wnt10a*, *Bcor*, *Dlx2* and others. Perhaps the more intriguing gene showing expression in the incisor pulp pericyte population was *Dspp*, a *bone fide* odontoblast differentiation gene (Fig. 3C). We could not detect expression of *Dspp* or other odontoblast-associated genes in any of the bone marrow pericyte samples sequenced (Fig. 3C). In contrast to dental pulp, bone marrow pericytes did

not show any expression of genes associated with osteogenic or other mesodermal cell differentiation. Thus expression of *Runx2, Sox9, Myf5, Pax3,* nor *Pparg* could be detected in bone marrow pericytes. Bone marrow pericytes did show over-representation of genes governing cell cycle progression and DNA replication (Fig. S3 A & B). A closer analysis of the datasets showed that core – enrichment was driven by genes encoding proteins that encode complexes involving cyclin dependent kinases, cyclins (Fig. S3 A') and essential DNA replication machinery (Fig. S3 B'). Bone marrow pericytes appear to be involved in regulating multiple arms of the immune response as they showed over – representation of gene clusters encoding proteins that are classically involved in signalling to B-cells, leukocytes and natural killer cells (Fig. S3 C & D). In addition they showed enrichment for genes involved in the regulation of inflammatory processes, IFNγ production and IL-1-mediated signalling (Fig. S3 E). Taking into account the strong enrichment of these bone marrow pericytes for haematopoietic and immune-related processes, we investigated if they correspond to the Nestin^{+} perivascular cells described by Mendez-Ferrer et al (del Toro et al., 2016; Méndez-Ferrer et al., 2010). What was seen was that these bone marrow pericytes do not express Nestin (*Nes*), or other neural crest associated genes such as *Snai1*, *Snai2*, *Sox9*, *Sox10 Pax3*, or *Foxd3*. In contrast, dental pulp pericytes show expression of *Nes*, *Snai1*, *Snai2* and *Sox9* (Fig. S4). These results being consistent with the well-known fact that pericytes in craniofacial structures are derived from cephalic neural crest, whilst pericytes in the trunk and bone marrow are of mesodermal derivation (Dellavalle et al., 2011; Etchevers, Vincent, Le Douarin, & Couly, 2001).

Epigenetic profiling identifies genomic loci in repressed, active or bivalent chromatin states. Having established that pericytes from different anatomical locations have dissimilar

transcriptomic outputs, a subset of which are unrelated with their blood vessel maintenance function, we set out to identify the molecular cause driving these transcriptomic differences. Whole genome epigenetic profiling using ChIP-seq was used to compare active (H3K4me3) and repressive (H3K27me3) histone marks on chromatin of the two freshly isolated pericyte populations. Global histone profiling confirmed the genome-wide distribution of enrichment peaks, with most peaks clustering within 500bp either side of the transcription start sites of protein coding genes (Fig. 4A). Gross comparisons of H3K4me3 and H3K27me3 enriched loci showed higher numbers for both histone modifications in bone marrow (Fig. 4B). Surprisingly, only 1050 loci of H3K4me3 and 1450 of H3K27me3 loci were shared by bone marrow and dental pulp pericytes (Fig. 4B). Gene ontology analysis of genes marked by H3K4me3 in the two cell populations showed common pathways enriched that confirmed the previously described RNA-seq datasets. These biological processes included basal metabolic regulation, ATP metabolism, transcriptional regulation and cell cycle progression (Fig. 4C). In addition, the bone marrow population showed higher enrichment of genes involved in the immune system, confirming status of genes previously identified to be expressed in the RNA-seq screen of these cells (Fig. 4C). H3K27me3 marked loci in both populations were enriched in genes modulating late stages of cell cycle progression, such as G2/M phase transition (Fig. 4C) and cytokinesis (Fig. 4D). Analysis for biological process enrichment of loci marked by H3K4me3 in both pericyte populations unsurprisingly identified processes that can be thought of as homeostatic. These collectively include the basal metabolic regulation of cells, transcriptional output regulation, and mRNA processing and degradation. One of the most significant pathways identified was heterophilic cell to cell adhesion which is consistent with the attachment of these cells to blood vessels (Fig. 4D). These H3K4me3 ChIP-seq results strongly mirrored the results obtained from the RNA-

seq datasets which conveyed the transcriptional status of these genes and identified them as being expressed in the pericyte populations from both organs (Fig. 2C). Contrastingly, repressive H3K27me3 marked loci shared by both populations targeted mitosis, cell growth and pro-apoptotic processes (Fig. 4D). We next wanted to compare on a global scale the overlap between the active/repressive histone landscapes in our cells with their respective RNA-seq datasets. Using an RNAseq specific GTF, we compared the histone landscapes of protein coding genes to the expression these genes had in the RNAseq datasets. The resulting coverage plots show that genes found to be expressed in pericytes from both organs overlap with genes high in H3K4me3. Contrastingly, very few genes were found to be expressed that were enriched for H3K27me3 in pericytes of either organ (Fig. 5A).

Many promoters and transcription start sites in the genome harbour both H3K4me3 and H3K27me3 and are termed bivalent (Voigt, Tee, & Reinberg, 2013). These chromatin marks localising at these genomic elements are thought to hold genes in a poised state that permits rapid gene activation, that in a cellular context might include genes involved in the initiation of cell differentiation (Roh, Cuddapah, Cui, & Zhao, 2006; Singh et al., 2015). Therefore, enrichment of loci marked by both histone modifications (bivalent loci) were analysed separately as such loci might identify “poised” genes that are ready to be transcribed as pericytes adopt a stromal stem cell identity. As with the monovalent loci, more bivalent enrichment peaks were observed in bone marrow cells compared to dental pulp, 1619 versus 1004 respectively (Fig. 5B) and only 385 of these were shared between the two cell populations (Fig. 5D). Enrichment analysis of bivalently marked genes in dental pulp showed that most of the genes marked are associated with regulating cell adhesion and transducing intracellular signals (Fig. 5C). Similarly, in bone marrow the same functional pathways were highlighted (albeit due to different genes) with the addition of genes

involved in mitosis and regulation of cell to cell signalling, neither of which showed enrichment in the dental pulp bivalent gene cluster (Fig. 5C). When considered in isolation, the 384 bivalently marked genes in both populations were enriched for biological processes involving cell adhesion, intracellular signal transduction and reorganising the chromatin environment (Fig. 5D). Percentage breakdowns of these genes into different biological processes showed that approximately 27% were involved in cellular regulatory processes (Fig. 5E), 62% of which are specific for cell to cell communication (Fig. 5E'). Taken together the transcriptomic and epigenomic datasets revealed that the epigenome of pericytes from two different locations reflects the function of the cells as MSC precursors.

Differential molecular programming drives in vitro differentiation in unstimulated monolayer cultures. The RNA-seq and ChIP-seq results outlined above argue that dental pulp-derived pericytes carry an odontogenic signature even before they have left blood vessels to become stromal stem cells. This conclusion was reached from the fact that not only do they express a number of genes known to be involved in odontogenesis, but also because of their low level expression of *Dspp*, an odontoblast differentiation gene (Chen et al., 2009; Wei, Ling, Wu, Liu, & Xiao, 2007). The low expression of *Dspp* was evident when investigating the ChIP-seq dataset for H3K4me3 which showed that dental pulp pericytes have a clear sharp peak of H3K4me3 at the *Dspp* transcription start site (*), indicating that transcription is taking place, something that is not observed in the bone marrow population (Fig. 6A). We next challenged these FACS sorted pericytes to see if they maintained a memory of origin when they were exposed to an *in vitro* environment under unstimulated culture conditions. After prolonged culture (31 days) we observed that *Dspp* expression was significantly upregulated in dental pulp pericytes as measured by qPCR (Fig. 6B). These bone

marrow pericytes did not upregulate *Runx2*, *Alp* or *Col2a1*. Similarly, bone marrow pericytes were subjected to the same in vitro assay and showed significant upregulation of *Runx2*, but not *Dspp* (Fig. 6D). This did not coincide with an upregulation of the adipogenic indicative gene *Pparg* or the chondrogenic indicative gene *Col2a1*. These cells did not upregulate a late osteogenic mineralisation gene *Ibsp* (Fig. 6D). To further characterise the underlying molecular cause for this *Runx2* specific upregulation, bone marrow pericyte ChIP-seq datasets were investigated. These showed that the *Runx2* transcription start site is bivalent as shown by the high enrichment of both H3K4me3 and H3K27me3 at that genomic region (Fig. 6E). In line with it being bivalent, *Runx2* expression could not be detected in fresh bone marrow pericytes when assayed using qPCR (Fig. 6D) or when evaluating the corresponding RNA-seq datasets. The ChIP-seq data indicated that this gene is held at a poised state, ready for subsequent activation when these cells are attached to blood vessels *in vivo*. Contrastingly, both *Pparg* and *Col2a* that were not upregulated in the *in vitro* assay are heavily enriched for repressive H3K27me3 *in vivo* (Fig. 6F). The late mineralization gene, *Ibsp,* whilst not expressed, is clear of any repressive H3K27me3 marks, suggesting that this gene is found in a chromatin environment making it amenable to transcription once the cognate transcription factors become available, whilst *Col2a1* and *Pparg* genes which are of inappropriate cell fates, are not.

PRC1 represses pericyte differentiation into inappropriate mesenchymal cell fates. It is widely accepted that Polycomb and Trithorax complexes safeguard proper differentiation of not only embryonic stem cells but also adult stem cells (Steffen & Ringrose, 2014). The PRC1 and PRC2 complexes play an active role in the deposition of repressive histone marks, namely H3K119u1 and H3K27me3 respectively via the Ring1b (PRC1) and Ezh2 (PRC2)

subunits. Contrastingly, trithorax family, Ash2L and Mll-containing complexes have methyl transferase activity and catalyse trimethylation of lysine 4 of histone 3 at multiple loci, thereby antagonising polycomb group- containing complexes (Di Croce & Helin, 2013; Shilatifard, 2012; Steward et al., 2006). To further characterise the epigenomic landscapes of these cells, and to identify what is contributing to this differentiation specificity (odontoblast vs osteoblast) on a molecular level, ChIP-seq datasets were generated for both pericyte populations for Ring1b, Ezh2, Ash2l and Mll1. When investigating their genome wide localisation, all complexes showed strongest association with the transcription start sites of protein coding genes (-1kb $\leq$ TSS $\leq$ 1kb) as expected (Fig. 7A). We wanted to determine to what degree these components shared similarities in the genomic loci they targeted, and if this indicated dissimilar epigenetic identities in these pericyte populations. Using principal component analysis on the generated ChIP-seq datasets we identified divergent chromatin landscapes in these pericytes. The datasets generated from the repressive PRC1 (Ring1b) and PRC2 (Ezh2) subunits in the dental pulp pericyte population clustered closely with the datasets of the H3K4me3 methyl transferases Ash2l and Mll1 derived from the bone marrow pericyte population (Fig. 7B). This would indicate that a high proportion of genomic regions repressed in the dental pulp pericyte population are active in the bone marrow population and *vice versa*. Overall the datasets generated from these complexes did not cluster together when comparing the two pericyte populations, indicating dissimilar euchromatin/heterochromatin landscapes and by association, gene expression of these cells *in vivo*.

PRC1 has been shown to bind H3K27me3 via its Cbx domain, whereby Ring1b can mono-ubiquitinate H3K119 and bring about chromatin compaction resulting in transcriptional repression (Boyle et al., 2010; Leeb & Wutz, 2007). Moreover, Ring1b has been shown to

participate in restricting cell differentiation by repressing inappropriate gene activation by localising to various lineage determining loci, and this repression is maintained during cell differentiation (Schuettengruber et al., 2009; van Arensbergen et al., 2013). A recent publication has shown that $CD146^{+}$ pericytes sourced from bone marrow are unable to form myofibers *in vitro* even when stimulated appropriately (Sacchetti et al., 2016), something that challenges the general dogma that pericytes are able to differentiate down myogenic, osteogenic, adipogenic and chondrogenic lineages when stimulated appropriately. In support of the former observation, Ring1b enrichment was investigated at three key transcription factor loci necessary for myogenic differentiation, *Myf5*, *Pax3* and *Myod1* (Cossu & Bianco, 2003; Montarras et al., 1991; Weintraub, 1993). We observed strong Ring1b enrichment at the transcription start sites of all three genes, in both pericyte populations (Fig. 7C). Subsequently, we investigated if bone marrow pericytes were endorsed to differentiate down chondrogenic or adipogenic pathways as widely described in the literature (Farrington-Rock et al., 2004). Surprisingly, a number of key chondrogenic induction genes show strong enrichment for Ring1b at their transcription start sites, including *Sox9, Osr1, Osr3, Runx3, Nfib, and Scx* (Briot et al., 2014; Gao, Lan, Liu, & Jiang, 2011; E.-J. Kim et al., 2013; Liu et al., 2013; Ng et al., 1997) (Fig. 7D). Similar results were obtained when investigating Ring1b localisation at genes necessary for adipogenic differentiation, such as *Cebp1* and *Cebpb* (Rosen & MacDougald, 2006) (Fig. 7E). Interestingly, adipogenic repressors *Cebpg*, and *Klf2* were devoid of a Ring1b localisation signal at their transcription start sites.

These genes were also shown to be expressed in bone marrow pericytes when investigating the corresponding RNA-seq datasets (Fig. 7E) suggesting that these bone marrow pericytes are molecularly obstructed from differentiating into adipocytes *in vivo*. The above results

indicate that neither of the pericyte populations analysed are readily myogenic *in vivo*, and in addition the bone marrow pericytes are molecularly restricted from differentiating down chondrogenic or adipogenic lineages.

Discussion

The XLacZ4 mouse line allowed us to efficiently isolate pericytes from bone marrow and dental pulp before they became stem cells since LacZ expression was never observed in stem cells or other cells not associated with blood vessels. These cells show all the previously recognised characteristics of pericytes, including contact with endothelial cell basement membrane. These two cell populations that share characteristics of high cell turnover and mineralised cell differentiation but differ in their location, embryonic origin (neural crest v mesoderm) and in the function as tissue-specific precursors of stromal stem cells, showed remarkably similar molecular characteristics. They both expressed a number of classical stem cell/pericyte marker genes including Thy1, Endoglin, CD146, Pdgfr-β in addition to less traditional markers such as SSEA-4 and Annexin A5, supporting previous reports (Feng, Mantesso, & Sharpe, 2010; Trost et al., 2016; Winkler, Bell, & Zlokovic, 2010; Bondjers et al., 2003; Winkler et al., 2010). Pericytes isolated from neither organ were 100% positive for any traditional pericyte markers, consistent with previous reports citing high heterogeneity of these cells *in vivo,* with respect to the cell surface markers they express (Kucia et al., 2007; Ozerdem, Grako, Dahlin-huppe, Monosov, & Stallcup, 2001). It still remains unclear to what extent differences in cell surface marker expression translate into functional heterogeneity in these cells. In all cases, similar percentages of $LacZ^{+}$ expressing cells were present, indicative of each isolated population being representative of pericytes. These $LacZ^{+}$ cells were always seen to be associated with blood vessels.

Intriguingly, none of our experiments could detect *Tbx18* expression in our pericytes and our data disagrees with the findings presented by Guimaraes-Camboa et al which identified *Tbx18*$^{+}$ perivascular cells in brain, heart, and adipose. According to Guimaraes-Camboa et al these Tbx18^{+} pericytes do not behave as MSCs *in vivo* (Guimarães-Camboa et al., 2017). We agree with a growing body of evidence arguing that more stringent evaluation of *Tbx18*$^{+}$ pericytes (also its suitability as a marker) is needed, ideally in organs that naturally remodel with age, before such claims can be unequivocally made (Campagnolo, Katare, & Madeddu, 2018; Cano, Gebala, & Gerhardt, 2017; Vishvanath, Long, Spiegelman, & Gupta, 2017; Wörsdörfer & Ergün, 2018).

RNA-seq profiling and expression analysis was carried out on fresh pericytes without a prior *in vitro* expansion step to identify any gene expression differences that could be present in pericytes before they have detached from blood vessels. ChIP-seq was subsequently performed on chromatin isolated from these cells using antibodies targeted to H3K4me3 and H3K27me3 to identify genomic loci that are found in euchromatin or heterochromatin enriched regions of the genome respectively. Not surprisingly, initial assessment of RNA-seq datasets showed that they were indicative of two cell populations with similar general features, as expected from the fact that they were isolated with the same specific marker. These features included, expression of housekeeping genes encoding proteins involved in mRNA production and degradation, cell adhesion and cell cycle regulation. Further characterisation of the gene expression profiles of pericytes from the two anatomical locations highlighted unexpected major differences. A major obvious difference between the two populations identified by both the RNA-seq and ChIP-seq datasets was that in the bone marrow pericyte population, there was a statistically strong over-representation for

genes involved in immune processes and genes encoding molecules widely described as regulators of the immune system. GSEA enrichment analysis confirmed that they showed enrichment in processes such as leukocyte activation and differentiation, B-cell receptor signalling, and NK cell regulation, with the majority of these genes found in transcriptionally amenable genomic loci as indicated by their enrichment for H3K4me3 and lack of H3K27me3. Perivascular cells identified as being Nestin^{+} and having a role in crosstalk with immune processes have previously been identified (Mendez-Ferrer et al. 2010), but Nestin was not found to be transcribed, nor in a region of euchromatin, in our datasets. Although it is well established that bone marrow stromal stem cells play an essential role in the maintenance of HSC populations, the extent to which they modulate immune processes *in vivo* is poorly understood (Abe et al., 2003; da Silva Meirelles, Caplan, & Nardi, 2008; Le Blanc & Mougiakakos, 2012). Our results suggest that an additional population of pericytes found in bone marrow that are Nestin^{-} may play an as of yet unidentified role in immune modulation. Something which cannot be said about their incisor dental pulp counterparts. A majority of these immune process governing genes were also identified as being in regions of euchromatin in the bone marrow pericyte population, as indicated by strong enrichment of H3K4me3 and lack of H3K27me3. In contrast, when analysing the RNA-seq datasets of incisor pericytes, we detected a clear odontogenic signature that was absent in their bone marrow counterparts. Gene ontology analysis on the upregulated genes showed that dental pulp pericytes express an overwhelming number of genes associated with odontogenesis none of which were expressed in bone marrow pericytes. This result was also confirmed when conducting a GSEA analysis on these datasets. One of the most significantly upregulated genes in the dental pulp pericyte population was *Dspp*, expression of which could not be detected in the bone marrow pericyte population using RNA-seq or qPCR.

Molecularly, at the transcription start site of *Dspp*, a sharp enrichment peak for H3K4me3 was identified in the corresponding dental pulp pericyte ChIP-seq dataset, something that was not observed in the bone marrow pericyte H3K4me3 dataset. A low level of *Dspp* expression in dental pulp pericytes was confirmed using qPCR on freshly isolated cells. Expression of the odontoblast differentiation gene in cells attached to blood vessels is surprising but in keeping with the high turnover rate of the continuously growing mouse incisor where MSCs have to provide a constant and rapid supply of new odontoblasts during homeostasis. Having MSC precursors ready "primed" for odontoblast differentiation may be a way of achieving this. Significantly, we were unable to detect *Dspp* expression in molar pulp pericytes via qPCR or RNAseq which is consistent with these cells being in a quiescent state during homeostasis and only required to provide cells for new odontoblast formation following dentine damage (data not shown) (Babb, Chandrasekaran, Carvalho Moreno Neves, & Sharpe, 2017). Overall, what was seen was that not only did ChIP-seq results mirror the gene expression patterns observed in the RNA-seq profiling, but also provided insight into the distinct chromatin architecture in these pericytes that is driving a corresponding transcriptional output. These major differences reflected aspects of pericyte identity as tissue resident MSC precursors.

Detailed analysis of the datasets of Polycomb Ring1b, Ezh2 and Trithorax Mll1, and Ash2l further indicated dissimilar epigenetic landscapes of these cells, as principal component analysis of these datasets shows that they differentially bind to loci depending on the origin of pericyte population. Both pericyte populations showed Ring1b enrichment at transcription start sites of genes needed to initiate myogenic differentiation indicating that neither of these cells are readily myogenic *in vivo*. The inability of MSCs to differentiate down the myogenic lineage was shown *in vitro* using bone marrow $CD146^{+}$ cells that failed

to make myofibres, although a molecular mechanism was not suggested (Sacchetti et al., 2016). In our bone marrow pericyte population Ring1b also localizes to transcription start sites of chondrogenic and adipogenic lineage specific genes, thereby mediating chromatin compaction of these loci. In contrast, adipogenic antagonists *Cebpg* and *Klf2* are expressed in these cells as shown by RNAseq. Thus certain differentiation pathways are specifically repressed in bone marrow at the level of chromatin organisation. Unlike the *Dspp* promoter in incisor dental pulp pericytes, the *Runx2* promoter in bone marrow pericytes is bound by both active and repressive histones and thus in a bivalent or poised state. This is supported by the absence of Runx2 transcripts (as assayed using RNA-seq and qPCR) in freshly isolated pericytes. However, when pericytes were isolated and placed in monolayer culture and expanded using unstimulating media, upregulation of *Runx2* expression was evident after 31 days. Significantly however, in these conditions, expression of chondrogenic nor adipogenic genes could be detected, consistent with their loci being marked only with repressive histones.

There has been a general belief that MSCs isolated from any tissue are equivalent, largely as a result of the definition proposed for MSCs (Castro-Malaspina et al., 1980; Moorman & Gerson, 2001; Prockop, 1997). *In vitro*, MSCs from different tissues do share expression of a number of similar pericyte marker genes (CD90, CD140b, CD105 etc) and all respond to similar cocktails of stimulatory factors and differentiate into mineralising cells (osteoblast- and chondrocyte-like cells) and fat cells (Brooke, Tong, Levesque, & Atkinson, 2008; Meirelles et al., 2008; Psaltis, Harbuzariu, Delacroix, Holroyd, & Simari, 2011). However, the composition of mineral produced by MSCs from different tissues varies widely and the expression of the various defining markers genes is not reproduced *in vivo* (Peister et al., 2004; Sacchetti et al., 2016; Sung et al., 2008; Volponi et al., 2015) The results presented

here clearly demonstrate that pericytes as stem cell precursors contain an epigenetic programme related to their future function as stem cells *in vivo*. We propose these programmes provide the cells with an intrinsic "memory" of their anatomical location that forms the basis for their restricted differentiation *in vivo*. Stimulation of differentiation *in vitro* presumably progressively erases some of this memory but the wide variations in the composition of mineral produced suggests some aspects of the memory are maintained. These observations have important consequences for any clinical use of heterotypic stem cells as cell sources to promote tissue regeneration and repair. What is also needed is to identify to what extent different subpopulations of pericytes (from the same organ) represent a lineage hierarchy and/or have functionally different roles *in vivo*. (Hardy et al., 2017)

Acknowledgements:

Authors would like to thank the BRC Flow Cytometry core at Guy's Hospital, and the Wellcome Trust Centre for Human Genetics at Oxford University for their services. Supported by MRC grant (MRK018035/1) and the Kings College NIHR/GSTFT Biomedical Research Centre. The authors declare no conflicts of interest.

References

Abe, K., Yarovinsky, F. O., Murakami, T., Shakhov, A. N., Tumanov, A. V, Ito, D., … Nedospasov, S. A. (2003). Distinct contributions of TNF and LT cytokines to the development of dendritic cells in vitro and their recruitment in vivo. *Blood*, *101*(4), 1477–1483. http://doi.org/10.1182/blood.V101.4.1477

Afgan, E., Baker, D., van den Beek, M., Blankenberg, D., Bouvier, D., Čech, M., … Goecks, J. (2016). The Galaxy platform for accessible, reproducible and collaborative biomedical analyses: 2016 update. *Nucleic Acids Research*, *44*(W1), W3–W10. http://doi.org/10.1093/nar/gkw343

Babb, R., Chandrasekaran, D., Carvalho Moreno Neves, V., & Sharpe, P. T. (2017). Axin2-expressing cells differentiate into reparative odontoblasts via autocrine Wnt/β-catenin signaling in response to tooth damage. *Scientific Reports*, *7*(1), 3102. http://doi.org/10.1038/s41598-017-03145-6

Bexell, D., Gunnarsson, S., Tormin, A., Darabi, A., Gisselsson, D., Roybon, L., … Bengzon, J. (2009). Bone marrow multipotent mesenchymal stroma cells act as pericyte-like migratory vehicles in experimental gliomas. *Molecular Therapy : The Journal of the American Society of Gene Therapy*, *17*(1), 183–190. http://doi.org/10.1038/mt.2008.229

Blankenberg, D., Von Kuster, G., Coraor, N., Ananda, G., Lazarus, R., Mangan, M., … Taylor, J. (2010). Galaxy: a web-based genome analysis tool for experimentalists. *Current Protocols in Molecular Biology / Edited by Frederick M. Ausubel ... [et Al.]*, *Chapter 19*, Unit 19.10.1-21. http://doi.org/10.1002/0471142727.mb1910s89

Boyle, S., Sproul, D., Eskeland, R., Leeb, M., Grimes, G. R., Gilbert, N., … Bickmore, W. A. (2010). Ring1B Compacts Chromatin Structure and Represses Gene Expression Independent of Histone Ubiquitination. *Molecular Cell*, *38*(3), 452–464. http://doi.org/10.1016/j.molcel.2010.02.032

Brachvogel, B., Moch, H., Pausch, F., Schlötzer-Schrehardt, U., Hofmann, C., Hallmann, R., …

Pöschl, E. (2005). Pervascular cells expressing annexin A5 define a novel mesenchymal stem cell-like population with the capacity to differentiate into multiple mesenchymal lineages. *Development*, *132*(11), 2657–2668. http://doi.org/10.1242/dev.01846

Brighton, C. T., Lorich, D. G., Kupcha, R., Reilly, T. M., Jones, A. R., & Woodbury, R. A. The pericyte as a possible osteoblast progenitor cell., Clinical orthopaedics and related research 287–299 (1992). http://doi.org/10.1097/00003086-199202000-00043

Briot, A., Jaroszewicz, A., Warren, C. M., Lu, J., Touma, M., Rudat, C., … Iruela-Arispe, M. L. (2014). Repression of Sox9 by Jag1 Is Continuously Required to Suppress the Default Chondrogenic Fate of Vascular Smooth Muscle Cells. *Developmental Cell*, *31*(6), 707–721. http://doi.org/10.1016/j.devcel.2014.11.023

Brooke, G., Tong, H., Levesque, J.-P., & Atkinson, K. (2008). Molecular trafficking mechanisms of multipotent mesenchymal stem cells derived from human bone marrow and placenta. *Stem Cells and Development*, *17*(5), 929–940. http://doi.org/10.1089/scd.2007.0156

Campagnolo, P., Katare, R., & Madeddu, P. (2018). Realities and misconceptions on the pericytes role in tissue repair. *Regenerative Medicine*, *13*(2), 119–122. http://doi.org/10.2217/rme-2017-0091

Cano, E., Gebala, V., & Gerhardt, H. (2017). Pericytes or Mesenchymal Stem Cells: Is That the Question? *Cell Stem Cell*, *20*(3), 296–297. http://doi.org/10.1016/J.STEM.2017.02.005

Castro-Malaspina, H., Gay, R. E., Resnick, G., Kapoor, N., Meyers, P., Chiarieri, D., … Moore, M. A. S. (1980). Characterization of Human Bone Marrow Fibroblast Colony-Forming Cells (CFU-F) and Their Progeny. *Blood*, *56*(2).

Chen, S., Gluhak-Heinrich, J., Wang, Y. H., Wu, Y. M., Chuang, H. H., Chen, L., … MacDougall, M. (2009). *Runx2, Osx* , and *Dspp* in Tooth Development. *Journal of Dental Research*, *88*(10), 904–909. http://doi.org/10.1177/0022034509342873

Cossu, G., & Bianco, P. (2003). Mesoangioblasts - Vascular progenitors for extravascular mesodermal tissues. *Current Opinion in Genetics and Development*, *13*(5), 537–542. http://doi.org/10.1016/j.gde.2003.08.001

Covas, D. T., Panepucci, R. A., Fontes, A. M., Silva Jr., W. A., Orellana, M. D., Freitas, M. C. C. C., … Zago, M. A. (2008). Multipotent mesenchymal stromal cells obtained from diverse human tissues share functional properties and gene-expression profile with CD146 + perivascular cells and fibroblasts. *Experimental Hematology*, *36*(5), 642–654. http://doi.org/10.1016/j.exphem.2007.12.015

Crisan, M., Yap, S., Casteilla, L., Chen, C.-W. C.-W., Corselli, M., Park, T. S., … Péault, B. (2008). A perivascular origin for mesenchymal stem cells in multiple human organs. *Cell Stem Cell*, *3*(3), 301–13. http://doi.org/10.1016/j.stem.2008.07.003

da Silva Meirelles, L., Caplan, A. I., & Nardi, N. B. (2008). In Search of the In Vivo Identity of Mesenchymal Stem Cells. *Stem Cells*, *26*(9), 2287–2299. http://doi.org/10.1634/stemcells.2007-1122

da Silva Meirelles, L., Chagastelles, P. C., & Nardi, N. B. (2006). Mesenchymal stem cells reside in virtually all post-natal organs and tissues. *Journal of Cell Science*, *119*(Pt 11), 2204–13. http://doi.org/10.1242/jcs.02932

del Toro, R., Chèvre, R., Rodríguez, C., Ordóñez, A., Martínez-González, J., Andrés, V., & Méndez-Ferrer, S. (2016). Nestin+ cells direct inflammatory cell migration in

atherosclerosis. *Nature Communications*, *7*, 12706. http://doi.org/10.1038/ncomms12706

Dellavalle, A., Maroli, G., Covarello, D., Azzoni, E., Innocenzi, A., Perani, L., … Cossu, Ǵ. (2011). Pericytes resident in postnatal skeletal muscle differentiate into muscle fibres and generate satellite cells. *Nature Communications*, *2*(1), 499. http://doi.org/10.1038/ncomms1508

Di Croce, L., & Helin, K. (2013). Transcriptional regulation by Polycomb group proteins. *Nature Structural & Molecular Biology*, *20*(10), 1147–1155. http://doi.org/10.1038/nsmb.2669

Diaz-Flores, L. J., Gutierrez, R., Madrid, J. . F., Varela, H., Valladares, F., Acosta, E., … Díaz-Flores, L. (2009). Pericytes. Morphofunction, interactions and pathology in a quiescent and activated mesenchymal cell niche. *Histology and Histopathology*, *24*(7), 909–969.

Dominici, M., Le Blanc, K., Mueller, I., Slaper-Cortenbach, I., Marini, F. C., Krause, D. S., … Horwitz, E. M. (2006). Minimal criteria for defining multipotent mesenchymal stromal cells. The International Society for Cellular Therapy position statement. *Cytotherapy*, *8*(4), 315–317. http://doi.org/10.1080/14653240600855905

Etchevers, H. C., Vincent, C., Le Douarin, N. M., & Couly, G. F. (2001). The cephalic neural crest provides pericytes and smooth muscle cells to all blood vessels of the face and forebrain. *Development*, *128*(7), 1059–1068.

Farrington-Rock, C., Crofts, N. J. J., Doherty, M. J. J., Ashton, B. A. A., Griffin-Jones, C., & Canfield, A. E. E. (2004). Chondrogenic and adipogenic potential of microvascular pericytes. *Circulation*, *110*(15), 2226–2232.

http://doi.org/10.1161/01.CIR.0000144457.55518.E5

Feng-Juan lv, Tuan, R. S., Cheung, K. M. C., & Leung, V. Y. L. (2014). The surface markers and identity of human mesenchymal stem cells. *Stem Cells*, 1–18. http://doi.org/10.1002/stem.1681

Feng, J., Mantesso, A., De Bari, C., Nishiyama, A., & Sharp, P. T. (2011). Dual origin of mesenchymal stem cells contributing to organ growth and repair. *Proceedings of the National Academy of Sciences of the United States of America*, *108*(16), 6503–6508. http://doi.org/10.1073/pnas.1015449108

Feng, J., Mantesso, A., De Bari, C., Nishiyama, A., Sharp, P. T., & Sharpe, P. T. (2011). Dual origin of mesenchymal stem cells contributing to organ growth and repair. *Proceedings of the National Academy of Sciences of the United States of America*, *108*(16), 6503–8. http://doi.org/10.1073/pnas.1015449108

Gang, E., Bosnakovski, D., & Figueiredo, C. (2007). SSEA-4 identifies mesenchymal stem cells from bone marrow. *Blood*, *109*(4), 1743–1751. http://doi.org/10.1182/blood-2005-11-010504.The

Gao, Y., Lan, Y., Liu, H., & Jiang, R. (2011). The zinc finger transcription factors Osr1 and Osr2 control synovial joint formation. *Developmental Biology*, *352*(1), 83–91. http://doi.org/10.1016/j.ydbio.2011.01.018

Goecks, J., Nekrutenko, A., & Taylor, J. (2010). Galaxy: a comprehensive approach for supporting accessible, reproducible, and transparent computational research in the life sciences. *Genome Biology*, *11*(8), R86. http://doi.org/10.1186/gb-2010-11-8-r86

Guimarães-Camboa, N., Cattaneo, P., Sun, Y., Moore-Morris, T., Gu, Y., Dalton, N. D., …

Evans, S. M. (2017). Pericytes of Multiple Organs Do Not Behave as Mesenchymal Stem Cells In Vivo. *Cell Stem Cell*, *20*(3), 345–359.e5. http://doi.org/10.1016/j.stem.2016.12.006

Hardy, W. R., Moldovan, N. I., Moldovan, L., Livak, K. J., Datta, K., Goswami, C., … March, K. (2017). Transcriptional Networks in Single Perivascular Cells Sorted from Human Adipose Tissue Reveal a Hierarchy of Mesenchymal Stem Cells. *STEM CELLS*, *35*(5), 1273–1289. http://doi.org/10.1002/stem.2599

Hellström, M., Kalén, M., Lindahl, P., Abramsson, A., & Betsholtz, C. (1999). Role of PDGF-B and PDGFR-beta in recruitment of vascular smooth muscle cells and pericytes during embryonic blood vessel formation in the mouse. *Development (Cambridge, England)*, *126*, 3047–3055.

Hematti, P., & Keating, A. (2010). *Mesenchymal Stromal Cells: Biology and Clinical Applications*. Humana Press. http://doi.org/10.1007/978-1-4614-5711-4

Huang, G. T.-J. T.-J., Gronthos, S., & Shi, S. (2009). Mesenchymal stem cells derived from dental tissues vs. those from other sources: their biology and role in regenerative medicine. *Journal of Dental Research*, *88*(9), 792–806. http://doi.org/10.1177/0022034509340867

Jiang, Y., Jahagirdar, B. N., Reinhardt, R. L., Schwartz, R. E., Keene, C. D., Ortiz-Gonzalez, X. R., … Verfaillie, C. M. (2002). Pluripotency of mesenchymal stem cells derived from adult marrow. *Nature*, *418*(6893), 41–49. http://doi.org/10.1038/nature00870

Kim, D., Langmead, B., & Salzberg, S. L. (2015). HISAT: a fast spliced aligner with low memory requirements. *Nature Methods*, *12*(4), 357–360. http://doi.org/10.1038/nmeth.3317

Kim, E.-J., Cho, S.-W., Shin, J.-O., Lee, M.-J., Kim, K.-S., & Jung, H.-S. (2013). Ihh and Runx2/Runx3 Signaling Interact to Coordinate Early Chondrogenesis: A Mouse Model. *PLoS ONE*, *8*(2), e55296. http://doi.org/10.1371/journal.pone.0055296

Kucia, M., Halasa, M., Wysoczynski, M., Baskiewicz-Masiuk, M., Moldenhawer, S., Zuba-Surma, E., … Ratajczak, M. Z. (2007). Morphological and molecular characterization of novel population of CXCR4+ SSEA-4+ Oct-4+ very small embryonic-like cells purified from human cord blood - Preliminary report. *Leukemia*, *21*(2), 297–303. http://doi.org/10.1038/sj.leu.2404470

Langmead, B., Trapnell, C., Pop, M., & Salzberg, S. L. (2009). Ultrafast and memory-efficient alignment of short DNA sequences to the human genome. *Genome Biology*, *10*. http://doi.org/10.1186/gb-2009-10-3-r25

Langmead, B., Trapnell, C., Pop, M., Salzberg, S. L., Down, T., Rakyan, V., … Reinert, K. (2009). Ultrafast and memory-efficient alignment of short DNA sequences to the human genome. *Genome Biology*, *10*(3), R25. http://doi.org/10.1186/gb-2009-10-3-r25

Le Blanc, K., & Mougiakakos, D. (2012). Multipotent mesenchymal stromal cells and the innate immune system. *Nature Reviews Immunology*, *12*(5), 383–396. http://doi.org/10.1038/nri3209

Leeb, M., & Wutz, A. (2007). Ring1B is crucial for the regulation of developmental control genes and PRC1 proteins but not X inactivation in embryonic cells. *Journal of Cell Biology*, *178*(2), 219–229. http://doi.org/10.1083/jcb.200612127

Liao, Y., Smyth, G. K., & Shi, W. (2014). featureCounts: an efficient general purpose program for assigning sequence reads to genomic features. *Bioinformatics*, *30*(7), 923–930.

http://doi.org/10.1093/bioinformatics/btt656

Liu, H., Lan, Y., Xu, J., Chang, C.-F., Brugmann, S. A., & Jiang, R. (2013). Odd-skipped related-1 controls neural crest chondrogenesis during tongue development. *Proceedings of the National Academy of Sciences of the United States of America*, *110*(46), 18555–60. http://doi.org/10.1073/pnas.1306495110

Love, M. I., Huber, W., & Anders, S. (2014). Moderated estimation of fold change and dispersion for RNA-seq data with DESeq2. *Genome Biology*, *15*(12), 550. http://doi.org/10.1186/s13059-014-0550-8

Meirelles, L. D. S., Caplan, A. I., Nardi, N. B., Eirelles, S. I. M., Aplan, A. R. I. C., Ance, N., … Nardi, N. B. (2008). In search of the in vivo identity of mesenchymal stem cells. *Stem Cells*, *26*(9), 2287–2299. http://doi.org/10.1634/stemcells.2007-1122

Méndez-Ferrer, S., Michurina, T. V, Ferraro, F., Mazloom, A. R., MacArthur, B. D., Lira, S. A., … Frenette, P. S. (2010). Mesenchymal and haematopoietic stem cells form a unique bone marrow niche. *Nature*, *466*(7308), 829–834. http://doi.org/10.1038/nature09262

Montarras, D., Chelly, J., Bober, E., Arnold, H., Ott, M. O., Gros, F., & Pinset, C. (1991). Developmental patterns in the expression of Myf5, MyoD, myogenin, and MRF4 during myogenesis. *The New Biologist*, *3*(6), 592–600.

Moorman, M., & Gerson, S. L. (2001). Phenotypic and Functional Comparison of Cultures of Marrow-Derived Mesenchymal Stem Cells (MSCs) and Stromal Cells, *66*(June 1997), 57–66.

Ng, L.-J., Wheatley, S., Muscat, G. E. ., Conway-Campbell, J., Bowles, J., Wright, E., … Koopman, P. (1997). SOX9 Binds DNA, Activates Transcription, and Coexpresses with

Type II Collagen during Chondrogenesis in the Mouse. *Developmental Biology*, *183*(1), 108–121. http://doi.org/10.1006/dbio.1996.8487

Ozerdem, U., Grako, K. A., Dahlin-huppe, K., Monosov, E., & Stallcup, W. B. (2001). NG2 proteoglycan is expressed exclusively by mural cells during vascular morphogenesis. *Developmental Dynamics*, *222*(2), 218–227. http://doi.org/10.1002/dvdy.1200

Peister, A., Mellad, J. A., Larson, B. L., Hall, B. M., Gibson, L. F., & Prockop, D. J. (2004). Adult stem cells from bone marrow (MSCs) isolated from different strains of inbred mice vary in surface epitopes, rates of proliferation, and differentiation potential. *Blood*, *103*(5), 1662–1668. http://doi.org/10.1182/blood-2003-09-3070

Phinney, D. G., & Sensebé, L. (2013). Mesenchymal stromal cells: misconceptions and evolving concepts. *Cytotherapy*, *15*(2), 140–5. http://doi.org/10.1016/j.jcyt.2012.11.005

Prockop, D. J. (1997). Marrow stromal cells as stem cells for nonhematopoietic tissues. *Science (New York, N.Y.)*, *276*(5309), 71–4. http://doi.org/10.1126/SCIENCE.276.5309.71

Psaltis, P. J., Harbuzariu, A., Delacroix, S., Holroyd, E. W., & Simari, R. D. (2011). Resident vascular progenitor cells-diverse origins, phenotype, and function. *Journal of Cardiovascular Translational Research*, *4*(2), 161–176. http://doi.org/10.1007/s12265-010-9248-9

Ramírez, F., Ryan, D. P., Grüning, B., Bhardwaj, V., Kilpert, F., Richter, A. S., … F., C. (2016). deepTools2: a next generation web server for deep-sequencing data analysis. *Nucleic Acids Research*, *44*(W1), W160–W165. http://doi.org/10.1093/nar/gkw257

Roh, T.-Y. T.-Y. T.-Y., Cuddapah, S., Cui, K., & Zhao, K. (2006). The genomic landscape of histone modifications in human T cells. *Proceedings of the National Academy of Sciences*, *103*(43), 15782–15787. http://doi.org/10.1073/pnas.0607617103

Rosen, E. D., & MacDougald, O. A. (2006). Adipocyte differentiation from the inside out. *Nature Reviews Molecular Cell Biology*, *7*(12), 885–896. http://doi.org/10.1038/nrm2066

Sacchetti, B., Funari, A., Remoli, C., Giannicola, G., Kogler, G., Liedtke, S., … Bianco, P. (2016). No Identical 'Mesenchymal Stem Cells' at Different Times and Sites: Human Committed Progenitors of Distinct Origin and Differentiation Potential Are Incorporated as Adventitial Cells in Microvessels. *Stem Cell Reports*, *6*(6), 897–913. http://doi.org/10.1016/j.stemcr.2016.05.011

Schuettengruber, B., Cavalli, G., Helness, A., Brookes, E., Pinho, S., Chandrashekran, A., … Azuara, V. (2009). Recruitment of Polycomb group complexes and their role in the dynamic regulation of cell fate choice. *Development*, *136*(21), 3531–3542. http://doi.org/10.1242/dev.033902

Shi, S., & Gronthos, S. (2003). Perivascular niche of postnatal mesenchymal stem cells in human bone marrow and dental pulp. *Journal of Bone and Mineral Research*, *18*(4), 696–704. http://doi.org/10.1359/jbmr.2003.18.4.696

Shilatifard, A. (2012). The COMPASS family of histone H3K4 methylases: mechanisms of regulation in development and disease pathogenesis, *81*(1), 65–95. http://doi.org/10.1146/annurev-biochem-051710-134100

Singh, A. M., Sun, Y., Li, L., Zhang, W., Wu, T., Zhao, S., … Dalton, S. (2015). Cell-Cycle Control

of Bivalent Epigenetic Domains Regulates the Exit from Pluripotency. *Stem Cell Reports*, *5*(3), 323–336. http://doi.org/10.1016/j.stemcr.2015.07.005

Steffen, P. a, & Ringrose, L. (2014). What are memories made of? How Polycomb and Trithorax proteins mediate epigenetic memory. *Nature Reviews. Molecular Cell Biology*, *15*(5), 340–56. http://doi.org/10.1038/nrm3789

Steward, M. M., Lee, J.-S., O'Donovan, A., Wyatt, M., Bernstein, B. E., & Shilatifard, A. (2006). Molecular regulation of H3K4 trimethylation by ASH2L, a shared subunit of MLL complexes. *Nature Structural & Molecular Biology*, *13*, 852–854. http://doi.org/10.1038/nsmb1131

Sung, J. H., Yang, H.-M., Park, J. B., Choi, G.-S., Joh, J.-W., Kwon, C. H., … Kim, S.-J. (2008). Isolation and Characterization of Mouse Mesenchymal Stem Cells. *Transplantation Proceedings*, *40*(8), 2649–2654. http://doi.org/10.1016/j.transproceed.2008.08.009

Tidhar, a, Reichenstein, M., Cohen, D., Faerman, a, Copeland, N. G., Gilbert, D. J., … Shani, M. (2001). A novel transgenic marker for migrating limb muscle precursors and for vascular smooth muscle cells. *Developmental Dynamics : An Official Publication of the American Association of Anatomists*, *220*(1), 60–73. http://doi.org/10.1002/1097-0177(2000)9999:9999<::AID-DVDY1089>3.0.CO;2-X

Trapnell, C., Roberts, A., Goff, L., Pertea, G., Kim, D., Kelley, D. R., … Pachter, L. (2012). Differential gene and transcript expression analysis of RNA-seq experiments with TopHat and Cufflinks. *Nature Protocols*, *7*(3), 562–578. http://doi.org/10.1038/nprot.2012.016

van Arensbergen, J., García-Hurtado, J., Maestro, M. A., Correa-Tapia, M., Rutter, G. A.,

Vidal, M., & Ferrer, J. (2013). Ring1b bookmarks genes in pancreatic embryonic progenitors for repression in adult β cells. *Genes & Development*, *27*(1), 52–63. http://doi.org/10.1101/gad.206094.112

Vidovic, I., Banerjee, A., Fatahi, R., Matthews, B. G., Dyment, N. A., Kalajzic, I., & Mina, M. (2017). α SMA-Expressing Perivascular Cells Represent Dental Pulp Progenitors In Vivo. *Journal of Dental Research*, 1–8. http://doi.org/10.1177/0022034516678208

Vishvanath, L., Long, J. Z., Spiegelman, B. M., & Gupta, R. K. (2017). Do Adipocytes Emerge from Mural Progenitors? *Cell Stem Cell*, *20*(5), 585–586. http://doi.org/10.1016/j.stem.2017.03.013

Voigt, P., Tee, W. W. W.-W., & Reinberg, D. (2013). A double take on bivalent promoters. *Genes and Development*, *27*(12), 1318–1338. http://doi.org/10.1101/gad.219626.113

Volponi, A. A., Gentleman, E., Fatscher, R., Pang, Y. W. Y., Gentleman, M. M., & Sharpe, P. T. (2015). Composition of Mineral Produced by Dental Mesenchymal Stem Cells. *Journal of Dental Research*, *94*(11), 1568–1574. http://doi.org/10.1177/0022034515599765

Wang, J.-M., Chen, A. F., & Zhang, K. (2016). Isolation and Primary Culture of Mouse Aortic Endothelial Cells. *Journal of Visualized Experiments : JoVE*, (118). http://doi.org/10.3791/52965

Wei, X., Ling, J., Wu, L., Liu, L., & Xiao, Y. (2007). Expression of Mineralization Markers in Dental Pulp Cells. *Journal of Endodontics*, *33*(6), 703–708. http://doi.org/10.1016/j.joen.2007.02.009

Weintraub, H. (1993). The MyoD family and myogenesis: Redundancy, networks, and thresholds. *Cell*, *75*(7), 1241–1244. http://doi.org/10.1016/0092-8674(93)90610-3

Wörsdörfer, P., & Ergün, S. (2018). Do Vascular Mural Cells Possess Endogenous Plasticity In Vivo? *Stem Cell Reviews and Reports*, *14*(1), 144–147. http://doi.org/10.1007/s12015-017-9791-8

Zhang, Y., Liu, T., Meyer, C. A., Eeckhoute, J., Johnson, D. S., Bernstein, B. E., … Brown, M. (2008). Model-based Analysis of ChIP-Seq (MACS). *Genome Biology*, *9*(9), R137. http://doi.org/10.1186/gb-2008-9-9-r137

Figures and figure legends

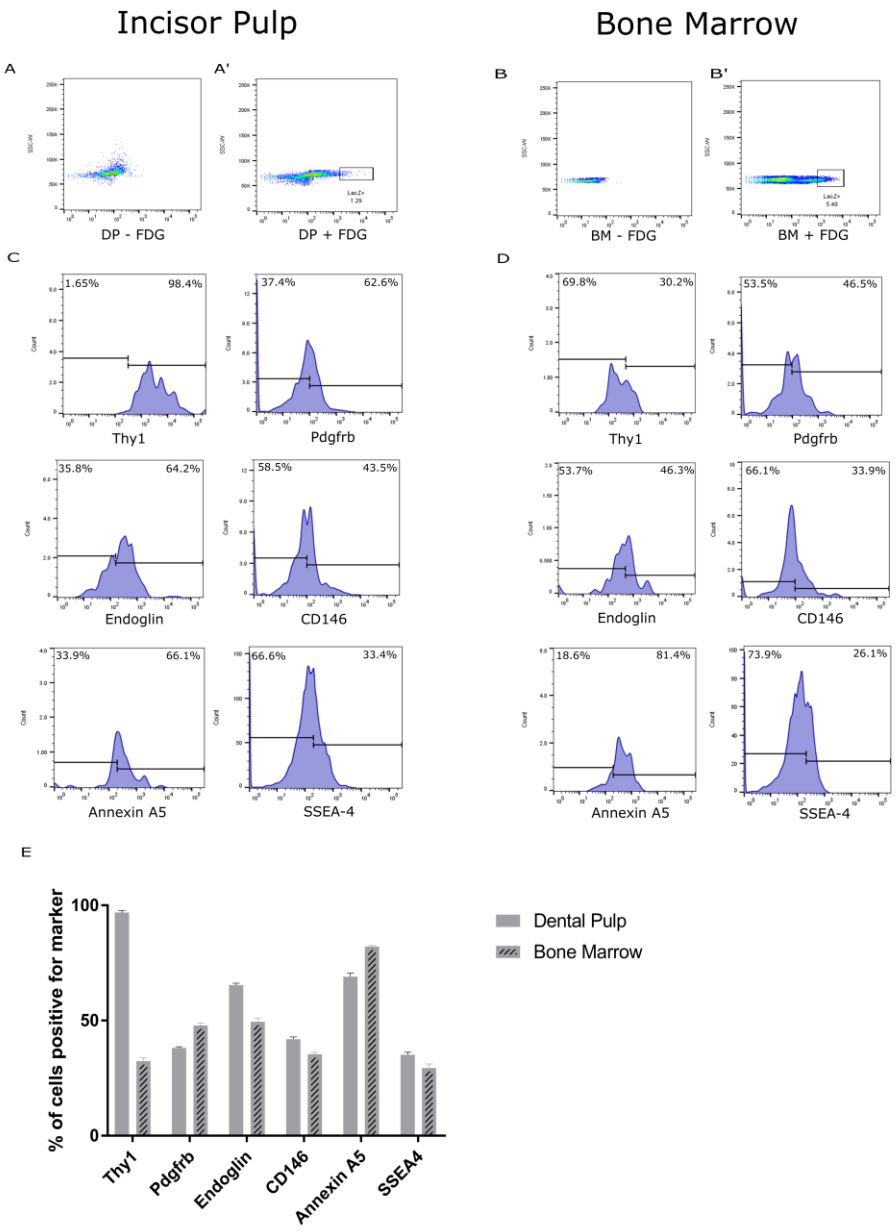

Figure 1: Flow cytometry analysis of pericytes. Single cell suspension of Collagenase D & Dispase digested incisor pulp, and bone marrow aspirate were analysed using a cell cytometer (A & B). Cell suspensions were fluorescently stained using FDG reagent and *LacZ+* pericytes were selected (A' & B'). *LacZ+* pericytes from both anatomical locations were analysed for a number of pericyte markers including Thy1, Pdgfrb, Endoglin, CD146, Annexin A5 and SSEA-4. Illustrative plots with percentages of positive and negative LacZ+ cells for

each marker are displayed (C & D). These percentages were consistent between non-littermates (n=5) as shown (E).

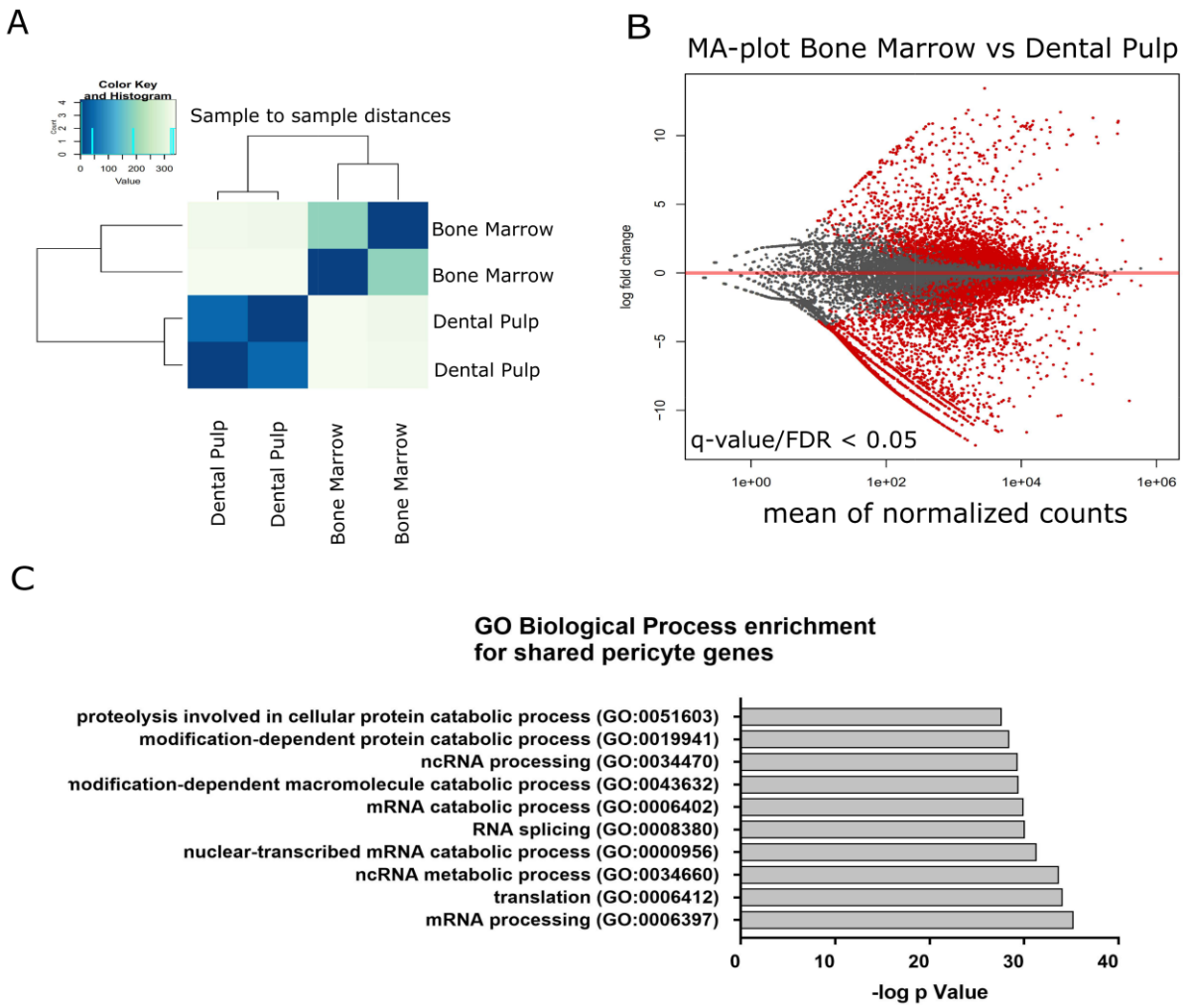

Figure 2: Bulk RNA-seq on pericyte population reveals diverging transcriptional landscapes. Two independent biological replicates were sequenced from each location to be used in RNA-seq analysis. Replicates show high degree of similarity between samples isolated from the same anatomical location (A). DESeq2 analysis detects differentially expressed genes between fresh pericytes isolated from incisor pulp vs those isolated from bone marrow. Approximately 850 genes are expressed exclusively in incisor pulp derived pericytes and 1000 in bone marrow derived pericytes. (C) Majority of genes detected (approximately 3500) were expressed by all pericytes. GO biological process enrichment analysis shows that

the top 10 hits for enriched pathways fall predominantly in regulating transcriptional output of cells and cell homeostatic processes.

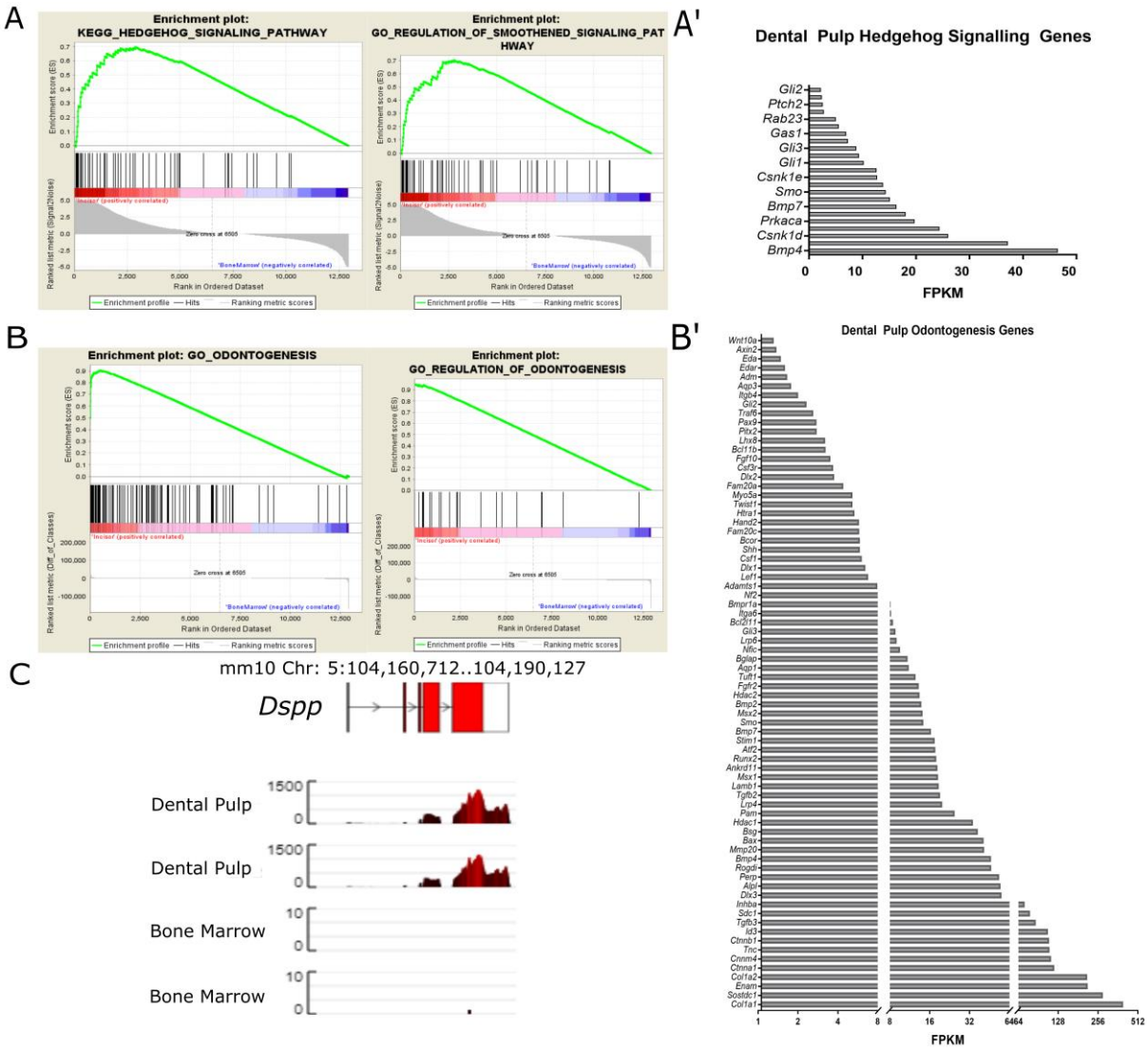

Figure 3: Pericytes isolated from incisor pulp are transcriptionally odontogenic like. GSEA analysis of genes detected using RNA-seq identifies an enrichment for genes involved in hedgehog signalling. This enrichment is detected only in pericytes isolated from dental pulp and not bone marrow (A). Top 10 genes driving this core enrichment are also shown with their respective normalised FPKM values as detected by RNA-seq (A'). GSEA analysis on significantly upregulated genes (q-value <0.05) detects core enrichment for genes involved in odontogenesis exclusively in the incisor pulp derived pericyte population (B) with the subsequent genes driving this enrichment shown (B'). *Dspp* expression was detected only in pericytes isolated from incisor pulp and not in those from bone marrow as shown by the

RNA-seq sequencing reads mapping to the *Dspp* locus (C). No reads could be detected in the bone marrow pericyte datasets.

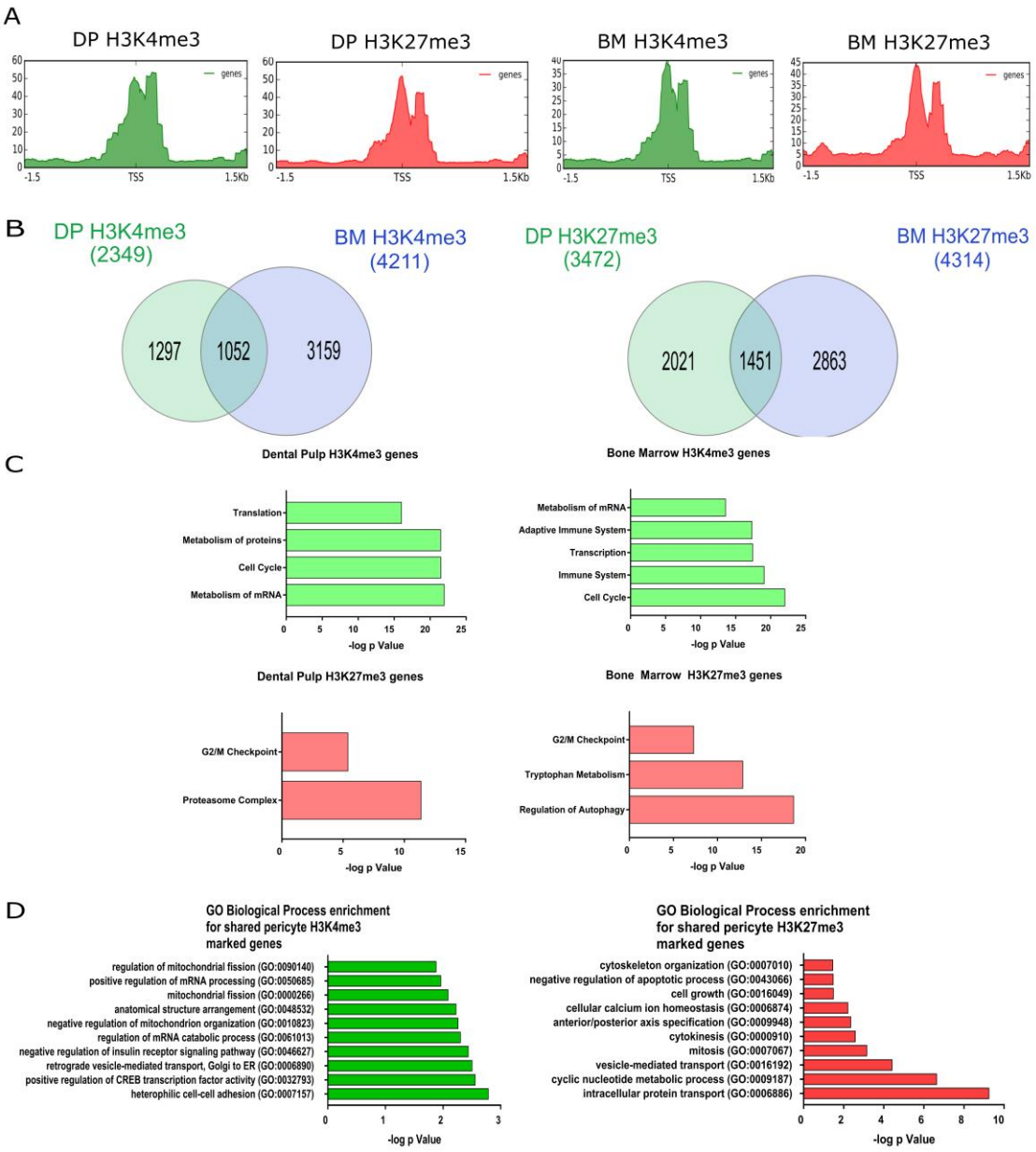

Figure 4: Epigenetic profiling of fresh pericytes. (A) Venn diagrams illustrating the overlap between the number of genes identified to have an enrichment peak for either H3K4me3 and H3K27me3 (TSS ± 500bp) in the two pericyte populations. Peak detection threshold was set to have a p-value < 0.005. (B) Global profiling of the selected histone marks shows that in both pericyte populations they enrich genomic regions overlapping and immediately upstream or downstream of gene transcription start sites (TSS ± 500bp). (C) Gene ontology analysis of genes marked by H3K4me3 in pericytes isolated from both anatomical locations

shows the high enrichment for genes involved in basal metabolic process, transcription regulation and also cell cycle progression. In addition, exclusively in the bone marrow pericyte population high enrichment for genes involved in immune system regulation are detected. In both populations genes encoding proteins involved in the G2/M phase of the cell cycle are enriched for H3K27me3. (D) Genes marked with the active histone mark H3K4me3 in both pericyte populations cluster in pathways involved in basal metabolic processes and also cell adhesion. Contrastingly, genes marked by the repressive histone mark H3K27me3 in both populations have significant hits in cell growth and proliferation. (DP : Dental pulp derived pericytes, BM: Bone marrow derived pericytes).

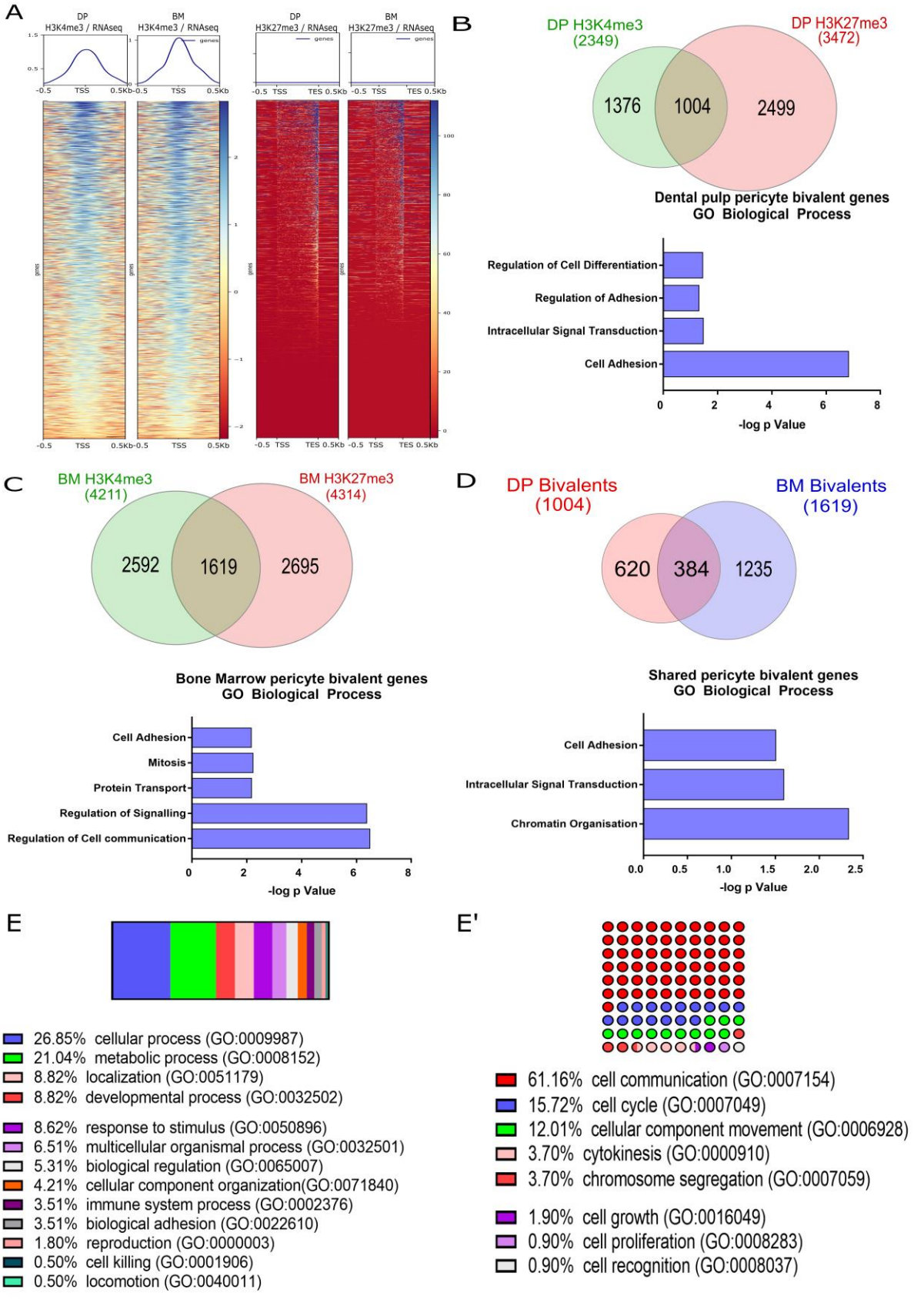
A
DP
H3K4me3 / RNAseq
BM
H3K4me3 / RNAseq
DP
H3K27me3 / RNAseq
BM
H3K27me3 / RNAseq
genes
-0.5 TSS 0.5Kb
TES 0.5Kb
B
DP H3K4me3
(2349)
DP H3K27me3
(3472)
1376
1004
2499
Dental pulp pericyte bivalent genes
GO Biological Process
Regulation of Cell Differentiation
Regulation of Adhesion
Intracellular Signal Transduction
Cell Adhesion
0
2
4
6
8
-log p Value
C
BM H3K4me3
(4211)
BM H3K27me3
(4314)
2592
1619
2695
Bone Marrow pericyte bivalent genes
GO Biological Process
Cell Adhesion
Mitosis
Protein Transport
Regulation of Signalling
Regulation of Cell communication
0
2
4
6
8
-log p Value
D
DP Bivalents
(1004)
BM Bivalents
(1619)
620
384
1235
Shared pericyte bivalent genes
GO Biological Process
Cell Adhesion
Intracellular Signal Transduction
Chromatin Organisation
0.0
0.5
1.0
1.5
2.0
2.5
-log p Value
E
26.85% cellular process (GO:0009987)
21.04% metabolic process (GO:0008152)
8.82% localization (GO:0051179)
8.82% developmental process (GO:0032502)
8.62% response to stimulus (GO:0050896)
6.51% multicellular organismal process (GO:0032501)
5.31% biological regulation (GO:0065007)
4.21% cellular component organization(GO:0071840)
3.51% immune system process (GO:0002376)
3.51% biological adhesion (GO:0022610)
1.80% reproduction (GO:0000003)
0.50% cell killing (GO:0001906)
0.50% locomotion (GO:0040011)
E'
61.16% cell communication (GO:0007154)
15.72% cell cycle (GO:0007049)
12.01% cellular component movement (GO:0006928)
3.70% cytokinesis (GO:0000910)
3.70% chromosome segregation (GO:0007059)
1.90% cell growth (GO:0016049)
0.90% cell proliferation (GO:0008283)
0.90% cell recognition (GO:0008037)

Figure 5: Bivalency in pericyte populations. (A) Coverage plots overlapping the specified histone mark with the relevant RNAseq dataset. As can be seen from the coverage plots, for both populations genes found to be expressed greatly overlapped with those detected to be decorated in H3K4me3. Contrastingly, expressed genes did not overlap with H3K27me3. Only protein coding genes were assessed that were taken from a UCSC obtained GTF file for mm10. (B) Venn Diagrams illustrating number of bivalent genes in incisor pulp (DP) and bone marrow (BM) pericytes, defined as genes enriched for both H3K4me3 and H3K27me3 at TSS±500bp. (C) Pericytes from incisor pulp and bone marrow share 384 bivalent genes. These genes cluster in biological processes regulating cell adhesion, signal transduction and chromatin organization (D). Percentage breakdown of shared bivalent gene contribution to different biological processes (E). Focusing on the cellular processes involved we see that ~62% of bivalent genes are involved in regulating cell communication (E').

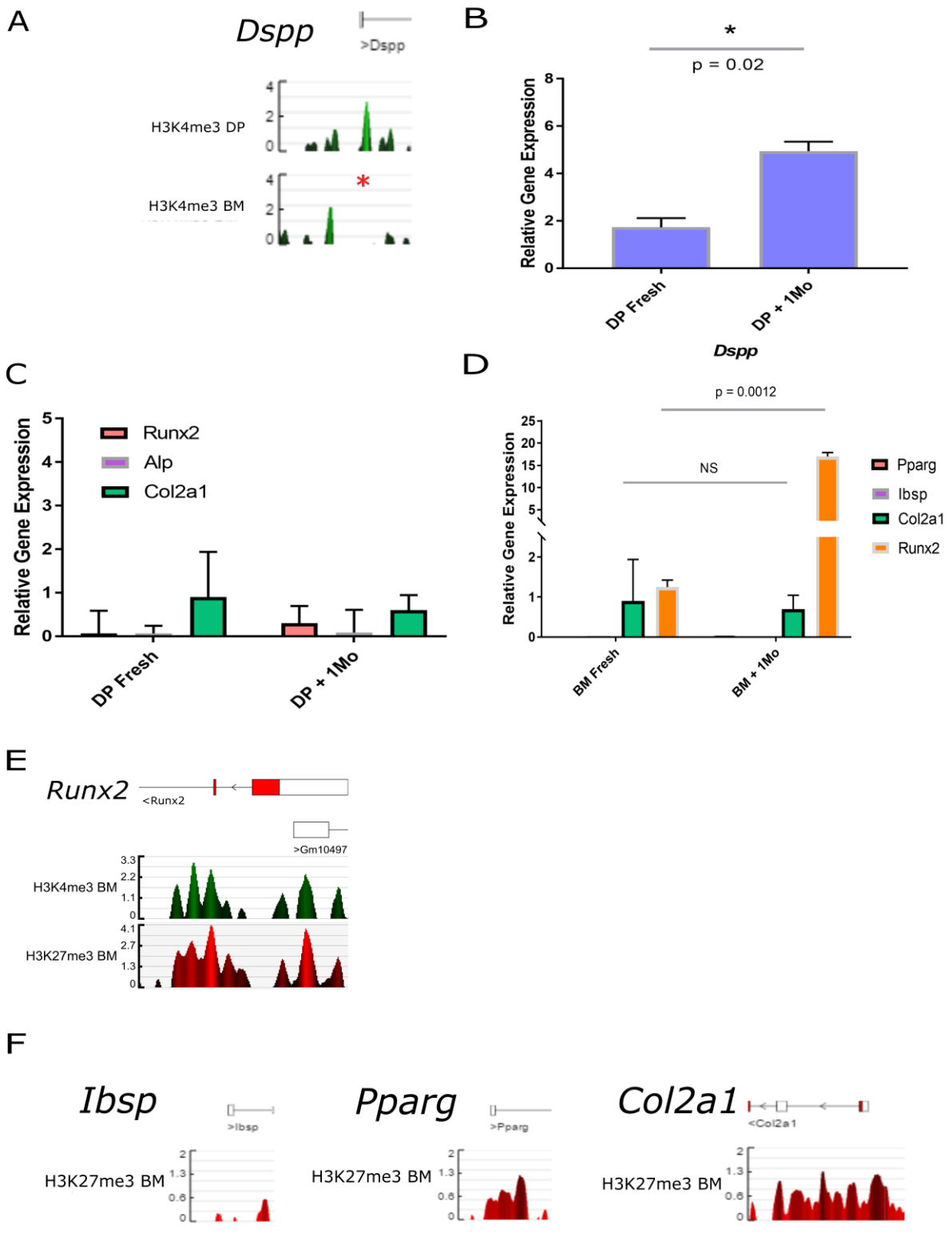

Figure 6: Pericytes as tissue specific, pre-programmed progenitors. The TSS of *Dspp* was investigated in the H3K4me3 ChIP-seq datasets, and a sharp peak was only detected in the

dental pulp pericyte population (A). Expression of *Dspp* in fresh dental pulp derived pericytes was validated by qPCR. Upon culturing these cells for 31 days in non-inductive medium *Dspp* expression was significantly upregulated (B). No significant changes of expression were observed for *Runx2*, *Alp* or *Col2a1* (C). Fresh pericytes isolated from bone marrow express low levels of *Runx2* and *Col2a1*. Upon culturing them in non-inductive media for 31 days Runx2 expression levels significantly increase while *Col2a1* levels remain unchanged. *Ibsp* and *Pparγ* could not be detected at the start or at the end point of the experiment (D). Investigating the *Runx2*- P2 TSS shows that it is bivalent with enrichment for both H3K4me3 and H3K27me3 histones (E). The TSS of *Ibsp*, *Pparg* and *Col2a1* were investigated for repressive histone marks and only those of *Pparg* and *Col2a1* were found to be enriched for H3K27me3. The *Ibsp* TSS was clear of this mark (F). (For qPCR data n=3 biological replicates, error bars represent SEM).

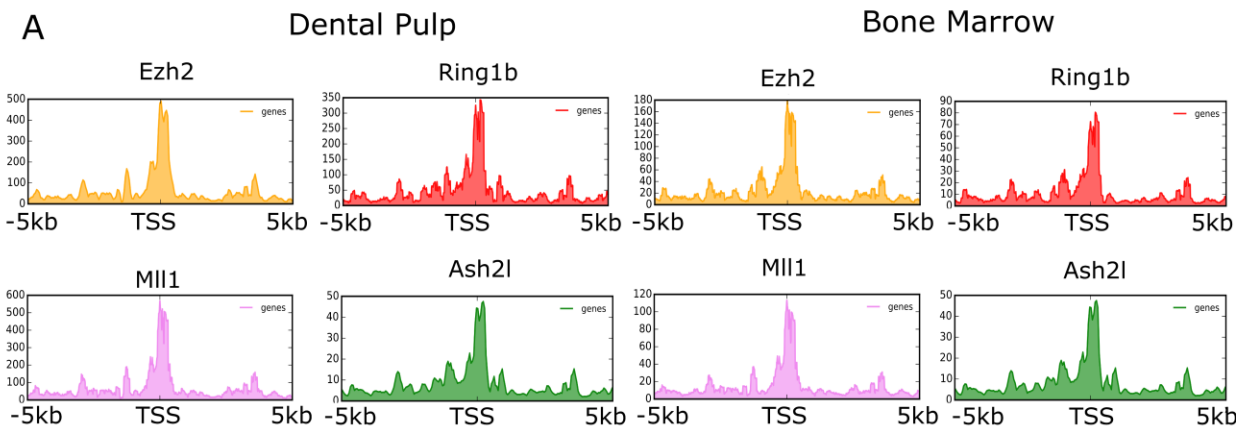
A
Dental Pulp
Bone Marrow
Ezh2
Ring1b
Mll1
Ash2l
genes
-5kb
TSS
5kb

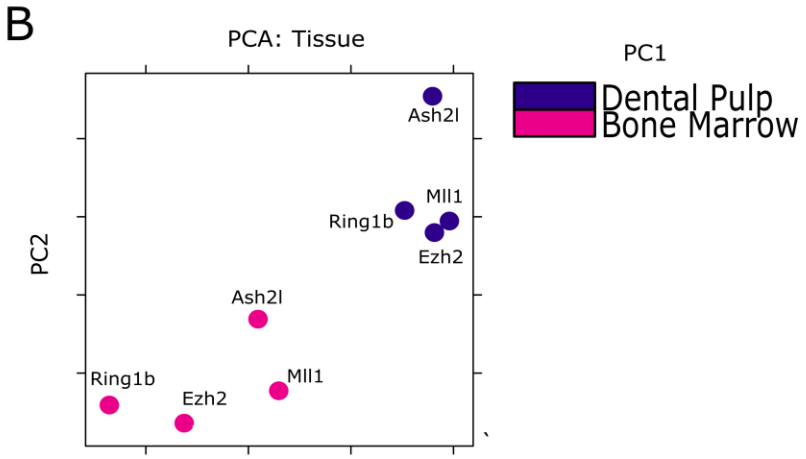
B
PCA: Tissue
PC1
PC2
Dental Pulp
Bone Marrow
Ash2l
Mll1
Ring1b
Ezh2

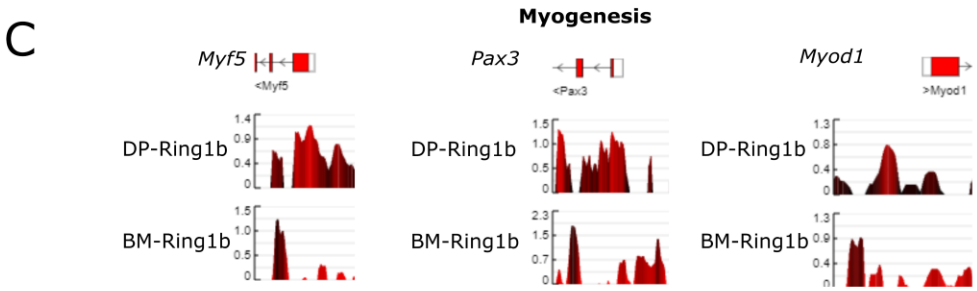
C
Myogenesis
Myf5
Pax3
Myod1
DP-Ring1b
BM-Ring1b

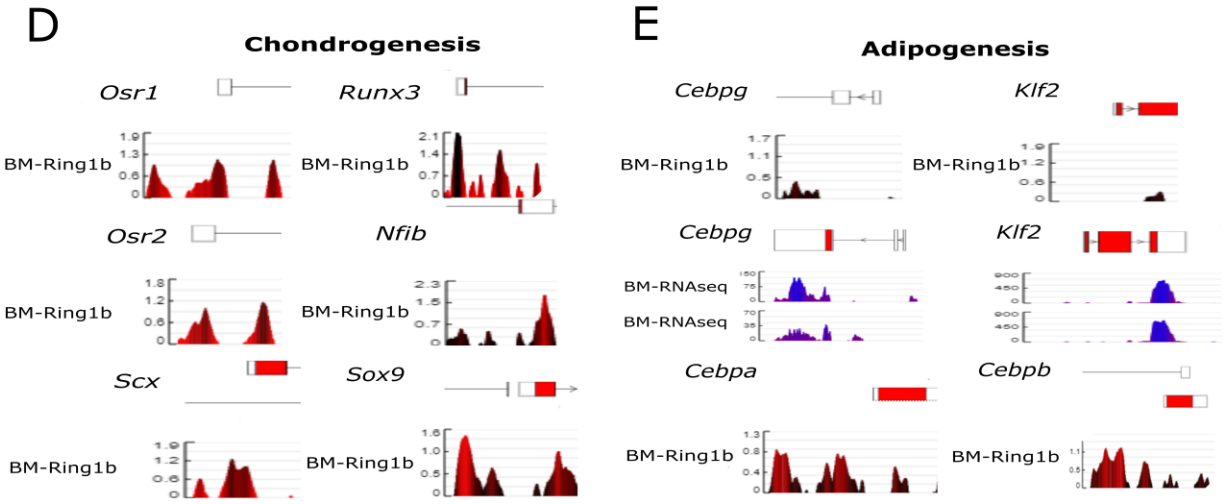
D
Chondrogenesis
Osr1
Runx3
Osr2
Nfib
Scx
Sox9
BM-Ring1b
E
Adipogenesis
Cebpg
Klf2
Cebpa
Cebpb
BM-Ring1b
BM-RNAseq

Figure 7: Dissimilar epigenetic landscapes in pericyte populations.

ChIP-seq was performed on the polycomb proteins Ezh2 (PRC2), Ring1b (PRC1), Mll1 and Ash2l. Enrichment peaks for these complexes were predominantly detected at the TSS of protein coding genes irrespective of pericyte population (A). Principal component analysis on the detected peaks showed that these datasets are very dissimilar when compared between dental pulp and bone marrow pericytes. Datasets of the transcriptional repressive complexes in dental pulp pericytes (Ring1b & Ezh2) are more similar in terms of where they localise in the genome with datasets obtained from Ash2l and Mll1 complexes in bone marrow. Ring1b represses inappropriate cell fates in vivo. Ring1b was found to localise at the TSS of genes mediating myogenesis, chondrogenesis and adipogenesis. In both pericyte population Ring1b enrichment is strong at the TSS of myogenic genes *Myf5*, *Pax3* and *Myod1* (C). In bone marrow pericytes Ring1b localises to the TSS of a number of genes needed to initiate and propagate chondrogenesis, including *Osr1, Runx3, Osr2, Nfib, Scx and Sox9* (D). Similarly, the same is true for adipogenic promoting genes *Cebpa* and *Cebpb*. Interestingly, Ring1b does not localise to adipogenic repressors *Cebpg* and *Klf2*. RNA-seq profiling shows that these two adipogenic repressors are strongly expressed in fresh pericytes in vivo (E).

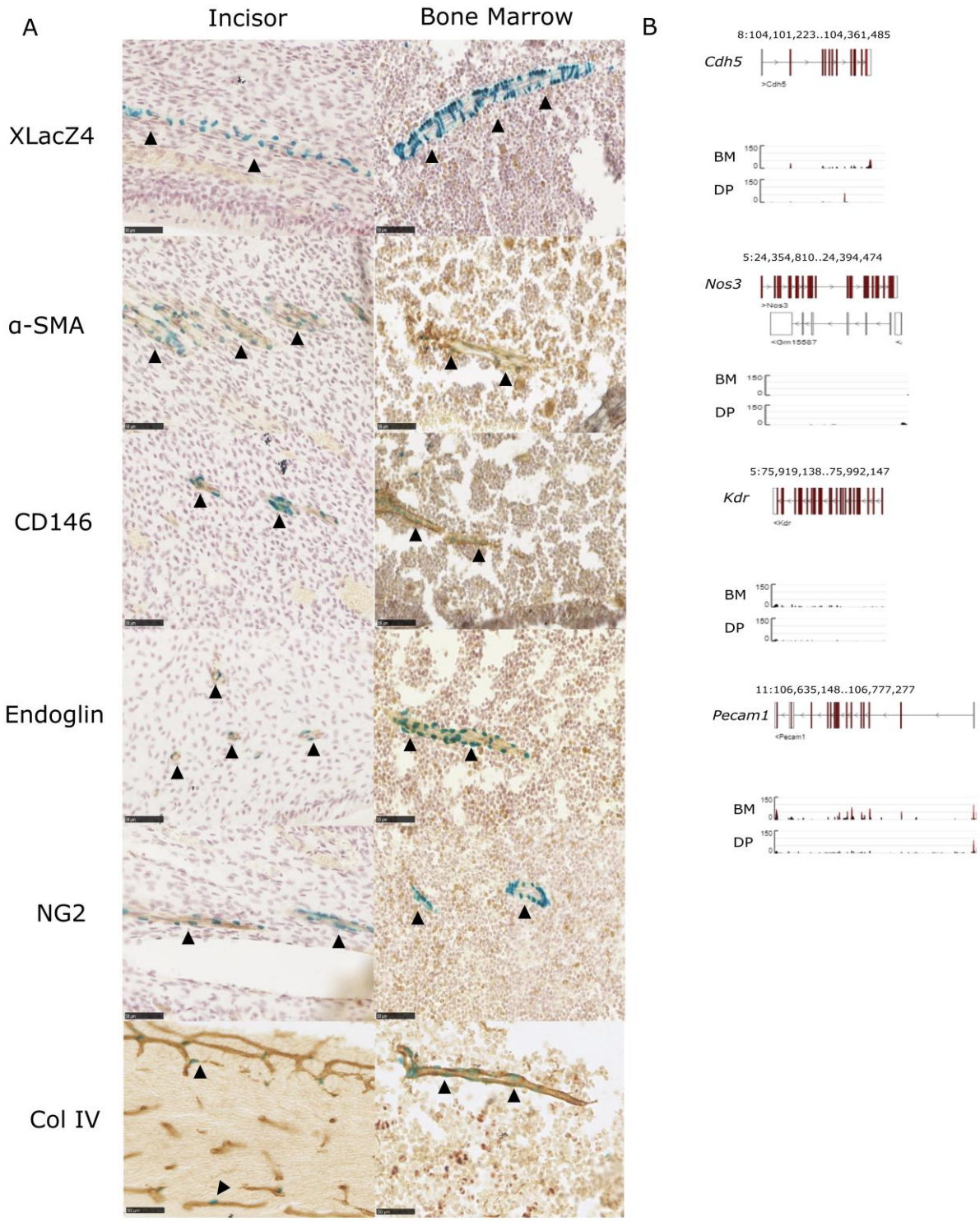

Supplementary 1: XLacZ4+ cells express canonical pericyte markers *in vivo*.

Tissue sections through incisor and bone marrow of XLacZ4 mice detecting *LacZ* expression using X-gal staining. LacZ+ cells are shown to be associated with blood vessels and co-express a number of markers classically associated with pericytes, including NG2, Cd146, Endoglin and α-SMA (A). Only very low of levels of NG2 could be detected in bone marrow LacZ+ cells. The expression of Collagen IV, a marker used to identify the basal lamina of endothelial cells was also visualised and found to localise adjacent to Xlaz4+ cells. We could not detect expression of traditional endothelial cell markers in these LacZ+ cells. Bulk RNA-seq performed on FACS isolated LacZ+ cells revealed very few reads aligning to the loci of *Cdh5*, *Kdr*, *Pecam1* or *Nos3* (B).

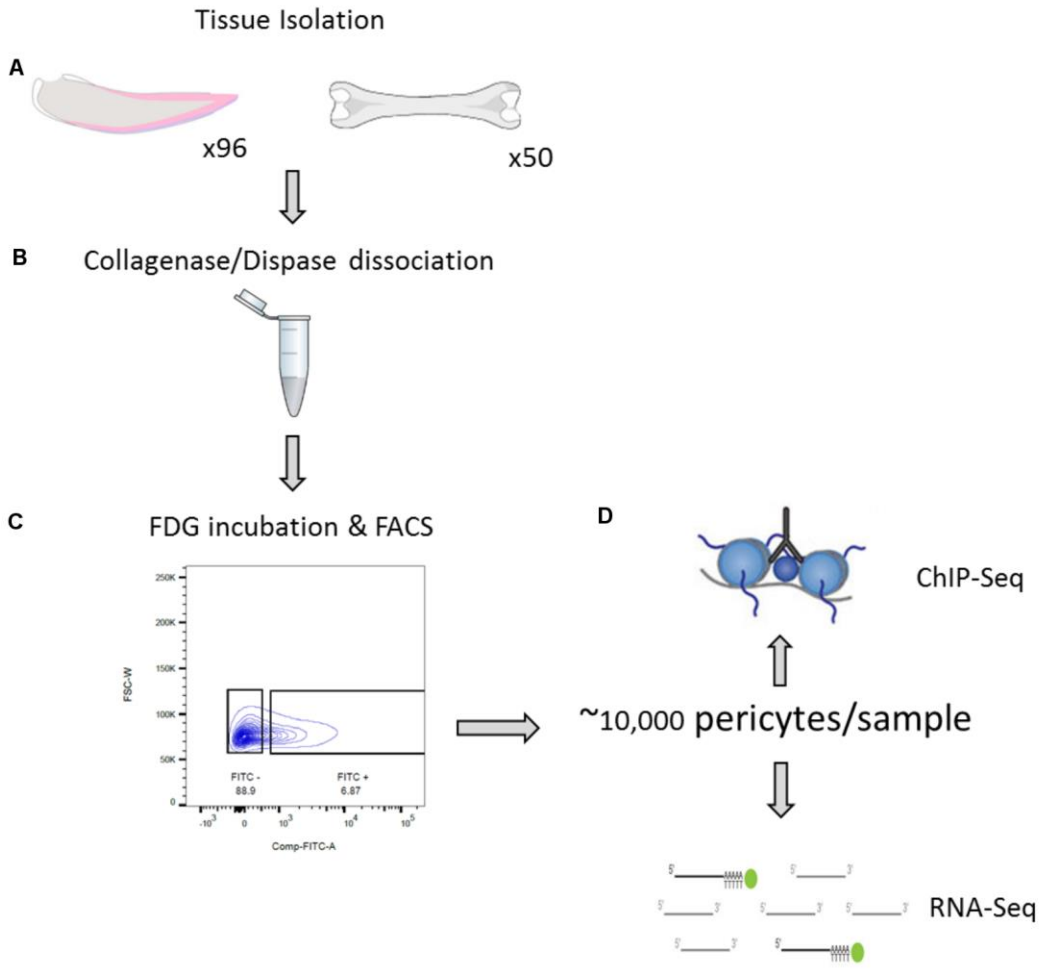

Supplementary Figure 2: Isolation of fresh pericytes for next generation sequencing.

A simple protocol was developed whereby *LacZ+* pericytes could be isolated from fresh tissue (incisors and tibia) of XLacZ4 transgenic mice at postnatal day 5 (A). Dental pulp was dissociated into a single cell suspension and bone marrow stroma was aspirated from the tibia (B). Cells were then incubated with FDG which fluorescently labels *LacZ+* cells and samples were then FACS sorted to isolate pericytes (C). These were then processed downstream for ChIP-seq and RNA-seq (D).

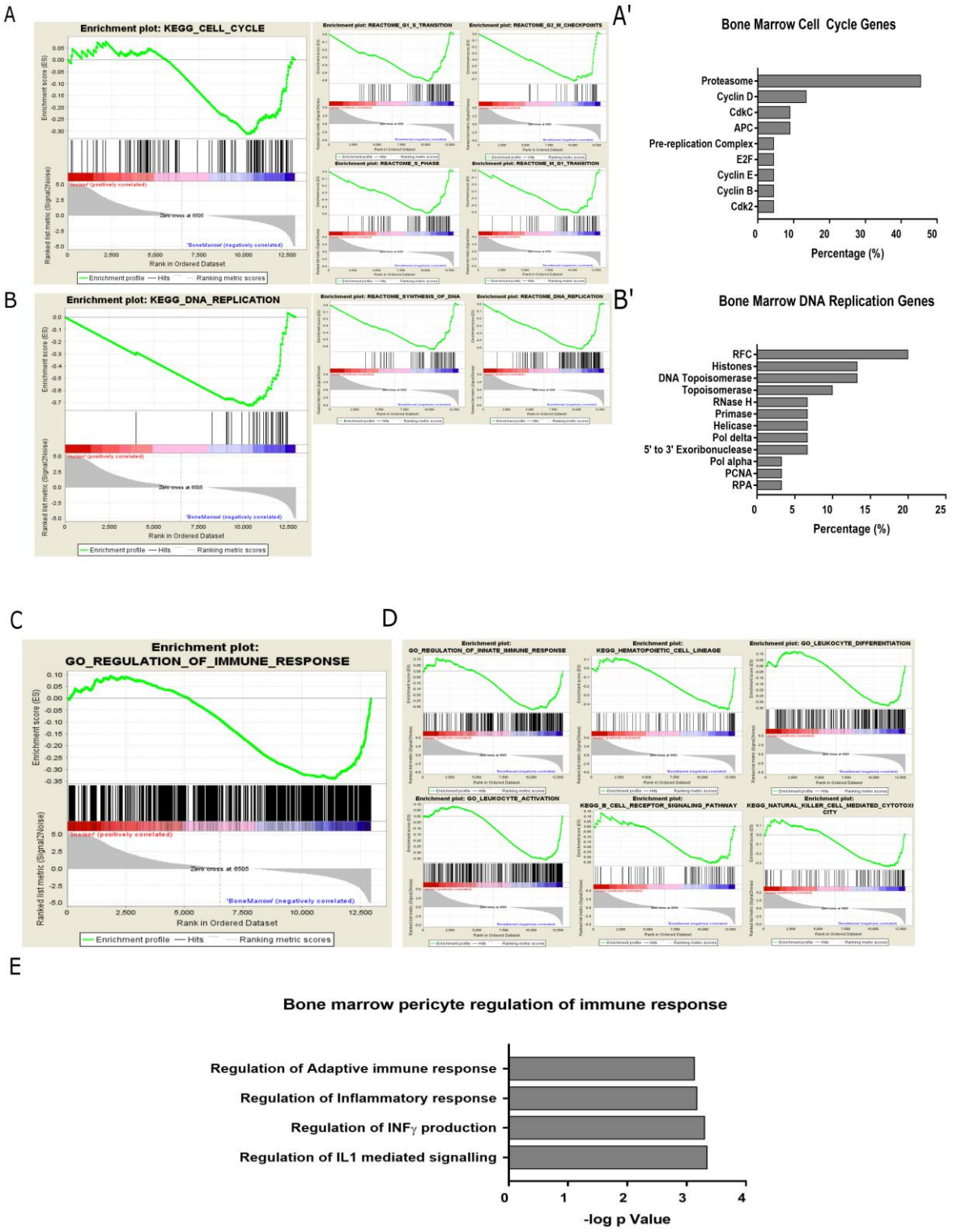

Supplementary Figure 3: GSEA analysis on bone marrow pericytes.

(A & B) GSEA enrichment analysis on genes significantly upregulated (q-value < 0.05) in the bone marrow pericyte population identifies over-representation of genes driving cell cycle and DNA replication were identified to be overabundant together with those modulating

various staged of the cell cycle. Those genes detected encode proteins that fall into a number of functionally important categories (A' and B'). GSEA analysis also suggests pericytes from bone marrow as being regulators of various arms of the immune system (C & D). Classical gene ontology enrichment analysis for the biological processes these genes influence also detects immune related pathways as being significantly overrepresented (E).

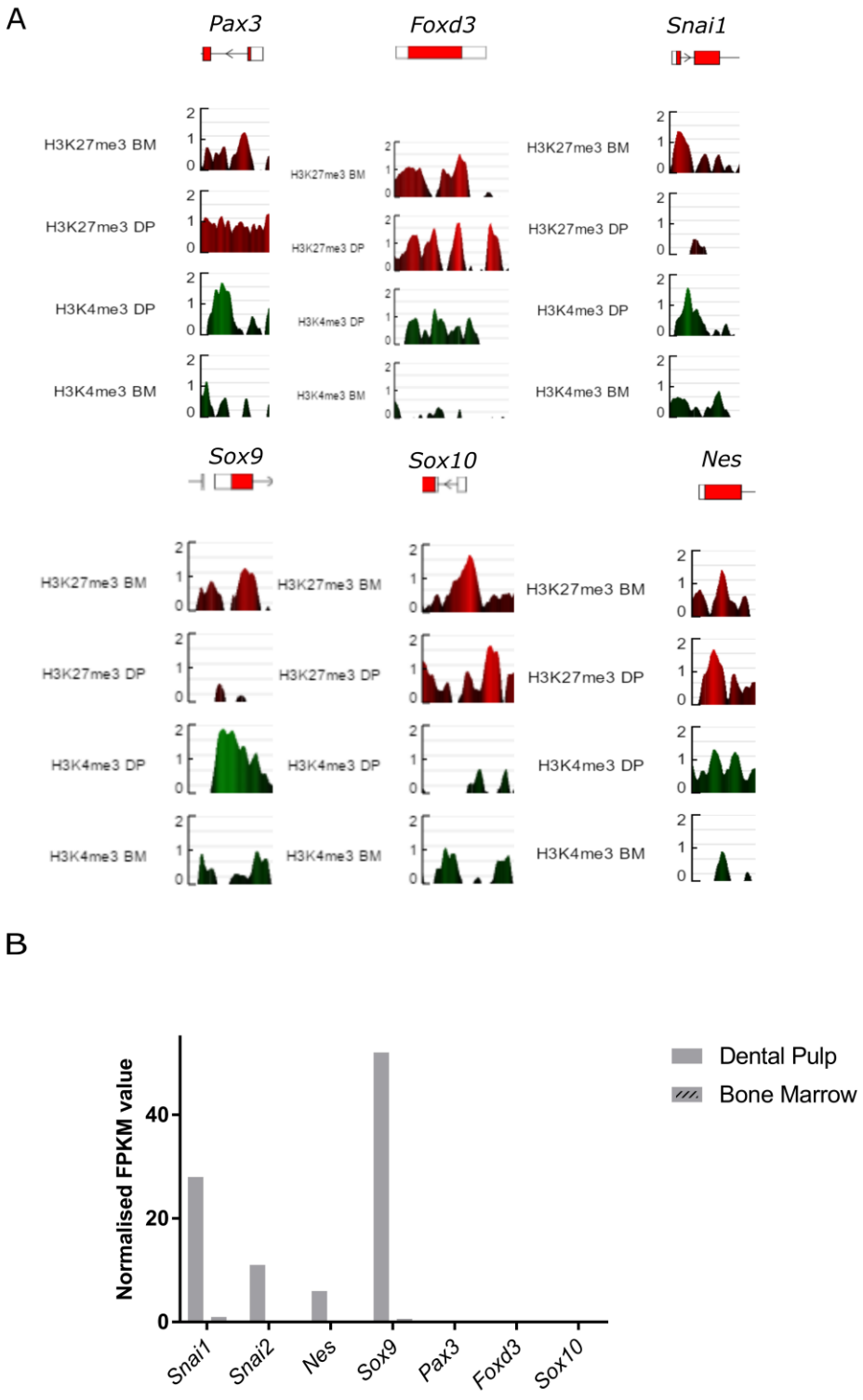

Supplementary 4: Neural crest gene profiling of pericyte populations.

Genome browser view of TSS of neural crest genes showing reads mapping for H3K4me3 & H3K27me3 in the two pericyte populations (A) All genes are abundant in repressive

H3K27me3 histone marks and absent of activating H3K4me3 histone marks in the bone marrow population. In contrast, dental pulp derived pericytes show enrichment of these marks at these TSS loci (A). Investigation of RNA-seq datasets showed that as expected, dental pulp derived pericytes express a number of these neural crest marker genes such as *Snai1*, *Snai2*, *Nes*, and *Sox9*, whilst their bone marrow counterparts do not (B).